Contrib Mineral Petrol (2007) 154:309–333
DOI 10.1007/s00410-007-0195-7

ORIGINAL PAPER

Petrology and geochemistry of eclogite xenoliths from the Rietfontein kimberlite, Northern Cape, South Africa

C. M. Appleyard · D. R. Bell · A. P. le Roex

Received: 22 April 2005 / Accepted: 26 February 2007 / Published online: 21 March 2007

Abstract Petrographic and geochemical features of a suite of eclogite xenoliths from the Rietfontein kimberlite that erupted through probable Proterozoic crust west of the Kaapvaal Craton in the far Northern Cape region of South Africa, are described. Group II eclogites dominate the suite both texturally and chemically, but can be subdivided into bimineralic, opx-bearing and kyanite-bearing groups. Temperature estimates from different geothermometers range from 700 to 1,000°C, indicating derivation from relatively shallow mantle depths. Orthopyroxene-bearing eclogites are inferred to originate from depths of 85 to 115 km and lie close to the average cratonic thermal profile for southern Africa. These uppermost mantle temperatures during the late Cretaceous provide evidence for equilibration of the off-craton lithosphere to craton-like thermal conditions following Namaqua-Natal orogenesis. The kyanite eclogites are distinct from the remaining eclogites in terms of both major and trace element compositions and their lesser degree of alteration. Garnets are richer in Ca, and are Cr-depleted relative to garnets from the bimineralic and opx-bearing eclogites, which tend to be more magnesian. Clinopyroxenes from the kyanite eclogites are more sodic, with higher Al_2O_3 and lower MgO contents than the bimineralic and opx-bearing eclogites. LREE-depletion, positive Sr and Eu anomalies, and the Al-rich, Si-poor bulk composition suggest a plagioclase-rich, probably troctolitic protolith for the kyanite eclogites. In contrast, the major and trace element bulk compositions of the high-MgO bimineralic and orthopyroxene-bearing eclogites are consistent with gabbroic or pyroxenitic precursors, or high-pressure cumulates, rather than mafic to ultramafic lavas. $\delta^{18}O$ values for garnets do not deviate significantly from typical mantle values. The observations reported do not discriminate unambiguously between continental and oceanic origins for the various eclogite components in the mantle lithosphere of this region.

Communicated by T.L. Grove.

C. M. Appleyard · D. R. Bell · A. P. le Roex (✉)
Department of Geological Sciences,
University of Cape Town,
Rondebosch 7700, South Africa
e-mail: anton.leroex@uct.ac.za

C. M. Appleyard
De Beers Geoscience Center,
Ormonde 2091, South Africa

D. R. Bell
Department of Chemistry and Biochemistry,
Arizona State University,
Tempe, AZ 85287-1604, USA

Introduction

Studies of deep-seated xenoliths and xenocrysts in kimberlites reveal a variety of lithologies that provide information on the constitution of the underlying crust and mantle. In favourable circumstances these xenoliths may be ordered in terms of their depth of origin to provide a stratigraphic section that can provide clues to the physical properties and geological history of the region. In addition, mineral thermometry can provide information on the local geotherm, or alternatively, physical conditions of metamorphism or magmatic crystallization.

The kimberlites of southern Africa carry to the surface xenoliths of lower crust and upper mantle origin that are dominated by coarse grained garnet peridotite, believed to represent the dominant upper mantle lithology. Other rock types occur in lesser abundance: these include other textural varieties of garnet peridotite, spinel peridotites, variously metasomatized peridotites, megacrysts, pyroxenites, eclogites and granulites (Gurney and Harte 1980). However, in certain kimberlites erupted through the Archean Kaapvaal craton (e.g. Roberts Victor, Bellsbank), eclogites of mantle origin dominate the xenolith suite. These concentrations and the high proportions of eclogitic components in the heavy mineral concentrates (xenocryst suites) of some of these kimberlites suggest that eclogites may locally approach 15% of the mantle column sampled by kimberlite (Schulze 1989). Some of this eclogite appears to be subducted oceanic crust (Jagoutz et al. 1984; MacGregor and Manton 1986; Shervais et al. 1988; Neal et al. 1990; Jacob et al. 1994; Viljoen et al. 1996; Jacob and Foley 1999; Jacob 2004) of Archean age (Kramers 1979; Pearson et al. 1995a; Richardson et al. 2001). This has important implications for the processes of craton root assembly and ancient continent stabilization (Shirey et al. 2001). Furthermore, some eclogites are rich in diamond, which lends economic importance to understanding their origin and distribution.

Abundant eclogite xenoliths have also been noted in kimberlites erupted through Proterozoic terranes bounding the Kaapvaal Craton to the west, and along the craton margins (e.g. Rickwood et al. 1969; Robey 1981; Pearson et al. 1995b; Schmitz and Bowring 2004), where they are commonly associated with mafic garnet granulites. This association is uncommon in cratonic xenolith assemblages (Griffin et al. 1979) though mafic lower crustal granulites do occur in relative abundance in some group II kimberlites (orangeites) of the northern Free State (Rickwood et al. 1969; Dawson and Smith 1987; Schmitz and Bowring 2003). The associated granulites and the equilibration pressures of 10–23 kbar (Robey 1981; Pearson et al. 1995b) for off-craton eclogites indicate that they are generally of shallower origin than their cratonic counterparts and derive predominantly from the lower crust and immediately adjacent mantle (Robey 1981; Pearson et al. 1995b). Comparatively few geochemical studies of such rocks have been undertaken, and as yet there is no evidence that the protoliths to these high pressure rocks share the ocean-floor history of some cratonic eclogites. Earlier studies favored formation of the mafic lower crust of eastern Namaqualand and Lesotho by underplating of mafic magmas during late Proterozoic Namaqua-Natal regional metamorphism. However, Schmitz and Bowring (2004) conclude on the basis of precise U–Pb geochronology and Sm–Nd isotope systematics that mafic granulite formation accompanied crustal thickening of Meso-Proterozoic and Paleao-Proterozoic protoliths of the Gordonia and Bushmanland subprovinces accreted to the Kaapvaal craton margin during the Namaqua-Natal event.

The Rietfontein kimberlite in the far Northern Cape province of South Africa is erupted well off the margin of the Kaapvaal craton through a poorly characterized crustal terrain known as the Rehoboth Subprovince (Hartnady et al. 1985). Much of the crust surrounding this terrain is considered to comprise continental fragments of varying Proterozoic ages, accreted to the Kaapvaal cratonic nucleus during the Proterozoic (Fig. 1). The xenoliths from this kimberlite are notable for their high proportion of eclogite, but without corresponding quantities of mafic granulite. This may signify a different origin from the eclogites that formed during high-grade metamorphism in the ~1 Ga Namaqua event (Rogers and Hawkesworth 1982; Schmitz and Bowring 2004), found elsewhere in kimberlites to the S and W of the craton. The aim of this study was to characterize the Rietfontein eclogites petrographically and chemically, to ascertain the depth and temperature of their origin, and to place constraints upon their possible mode of origin. The results provide a rare window to the crust and underlying mantle of the enigmatic Rehoboth Subprovince, and have implications for their structure and origin, as discussed further in this paper.

The Rietfontein kimberlite and xenoliths

The Rietfontein kimberlite is located at 26.75°S, 20.04°E, approximately 2 km east of the South Africa–Namibia border in the Northern Cape province of South Africa (Fig. 1). This is ~200 km west of the inferred margin of the Kaapvaal craton (Fig. 1) in an area where Kalahari sands and Karoo-age sedimentary rocks obscure the nature of crystalline basement. The kimberlite, discov-

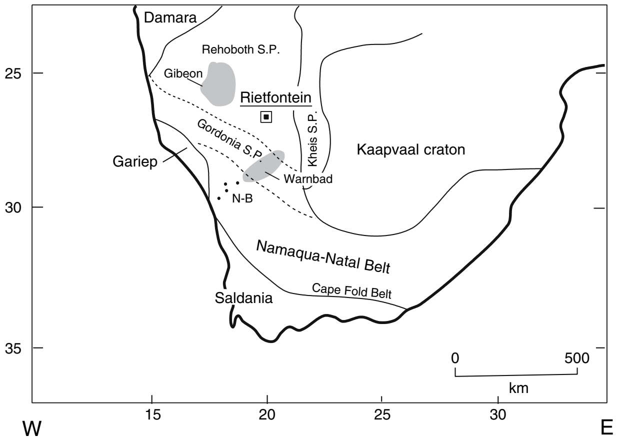

Fig. 1 Southern Africa showing location of the Rietfontein kimberlite in relation to the approximate boundaries of the Kaapvaal craton, the Namaqua-Natal Belt and the Rehoboth subprovince. Approximate locations of spatially associated kimberlite/melilitite clusters, Gibeon, Warmbad and Namaqualand-Bushmanland (N-B), are shown for comparison

ered in the early 1900s is comprised of a pipe, approximately 2 ha. in surface area, and an associated dyke extending almost 1.5 km in a north-easterly direction. The pipe has been repeatedly prospected over a long period, but is believed to lack diamond (Gurney 1984; Dawson 1989).

Rietfontein is one of five or so kimberlites known from this region, referred to in early literature as Gordonia. None has been well studied or described in any detail. The Gordonia kimberlites (Rietfontein, Noenieput, Witkop groups of intrusions) occur at the northeastern end of an array of melilitite and kimberlite clusters that includes (from SW to NE) the Garies melilitites, the Gamoep melilitites, the Pofadder kimberlites and the Warmbad province kimberlites. U–Pb dating of zircons derived from the Rietfontein kimberlite yielded ages of 71.9 and 71.1 Ma (Davis et al. 1976). This is slightly younger than the Hoedkop melilitite (75 Ma) of the Gamoep cluster (Janney et al. 2002) but some 5–10 m.y. older than other Garies and Gamoep melilitites (Davis et al. 1976). It is within the range of ages determined for kimberlites and associated alkaline intrusions of the Gibeon-Gross Brukkaros Province, some 200 km to the west in Namibia (Kurszlaukis et al. 1998; Davies et al. 2001). The Rietfontein kimberlite is a typical group I variety, consisting of olivine and other mantle derived macrocrysts set in a matrix containing serpentine, phlogopite, calcite and monticellite pseudomorphs.

The mantle derived component in the Rietfontein kimberlite consists of eclogite, peridotite and websterite xenoliths, not normally exceeding 10 cm in diameter, with most appreciably smaller. Notable among the suite are occasional spectacular fresh, kyanite-bearing eclogites. The pipe is deeply weathered over much of its exposed surface and it is likely that the proportions of the larger types of xenoliths, which are dominated by the eclogite–websterite suite, are influenced by weathering of olivine and enstatite that would lead to the disintegration of peridotite xenoliths. The heavy mineral concentrate from the pipe is rich in chrome diopside and pyrope, and is furthermore characterized by large (up to 1 cm) rutile macrocrysts.

Despite its discovery in 1913, the kimberlite and its xenoliths have been little studied. Petrographic characteristics of kyanite-bearing eclogites, including major element analyses of four samples, were recorded by Gurney et al. (1971), and the hydroxyl and major element compositions of garnets from ten Rietfontein eclogites were analysed by Bell and Rossman (1992). Gurney (1984) presented data on garnet macrocrysts from the heavy mineral concentrate. The present study thus constitutes the first systematic studies of xenoliths from this kimberlite or from any other in the region.

Methods

Forty-seven eclogite xenoliths collected from the Rietfontein kimberlite were examined in this study. Twenty-nine samples (those labelled JJG, PC and Rftn) were selected from the research collection at the University of Cape Town, and a further 18 samples (labelled CMA) were collected from old concentrate dumps and kimberlite spoil heaps. Most samples were between 1 and 5 cm in diameter but two larger samples measured 6 and 10 cm in diameter. The larger samples are all rounded and ellipsoidal in shape, whereas the smaller samples exhibit more angular and irregular shapes and are probably the remnants of larger weathered and broken samples.

Double-polished probe sections were prepared from the eclogite hand specimens for petrographic description and electron microprobe analysis. Subsequent LA-ICP-MS analyses were conducted on grain mounts of separated clinopyroxene and garnet. The major element compositions of garnet, clinopyroxene and accessory minerals from the Rietfontein eclogites were determined at the University of Cape Town using the Cameca-Camebax electron microprobe operating at 40 nA cup current and an accelerating voltage of 15 kV. Ten second counting times at peak and background positions were used for all elements, except Na in garnet and K in clinopyroxene, for which counting times of 30 s were used. Data were reduced online using the PAP reduction method, as described by Pouchou and Pichoir (1991). In each eclogite sample, at least two grains of each of the primary minerals were analysed, and each grain was analysed at least twice, with core and rim analyses being obtained where possible. Fe^{3+} contents were calculated for ilmenite using the method of Droop (1987). Rietfontein garnet data from Bell and Rossman (1992) are included in the plots in order to expand the analytical database.

Concentrations of 16 trace elements (REE, Th, Nb, Sr, Zr, Y, Sc and Ni) of the silicate minerals were determined in situ by LA-ICPMS at the University of Cape Town. The instrument used was a Perkin Elmer Elan 6000 ICP-MS coupled to a Cetac LSX-200 laser ablation module using a 266 nm frequency-quadrupled Nd-YAG laser. A typical analysis consisted of three replicates of 100 readings each, with each replicate representing one sweep of the mass range. The counting time for one sample was typically 60–100 s. Every hour three replicates of 100 readings were counted on the Argon carrier gas alone to establish the background. The NIST 610 and 612 glass standards were used to calibrate relative element sensitivities and each analysis was normalized using Si values determined by electron microprobe. Calculated detection limits using the gas blank range from 10 to 20 ppb for REE, Th, Nb, Sr, Zr and Y, 100 ppb for Sc and 2 ppm for Ni. The typical precision and accuracy ranged from 1 to 10%.

Oxygen isotope analyses were performed using a laser fluorination technique and Finnigan MAT 252 stable isotope mass spectrometer at the University of Cape Town. Details of the technique have been described by Harris et al. (2000); reproducibility in the current study can be gauged from the repeat analysis of an in-house standard (MON-GT) which gave an average value of 5.55 ± 0.15‰ ($n = 3$) relative to SMOW.

For geothermometry, core and rim compositions were averaged separately. All Fe was assumed to be Fe^{2+}. These compositional averages for garnet, clinopyroxene and orthopyroxene were then used to calculate equilibration temperatures and pressures (where possible) using the Macintosh-based FORTRAN program TP97v.2 (Smith 1999) and a self-designed Excel spreadsheet.

Petrography of the eclogites

The eclogites were divided on the basis of their dominant primary mineralogy into three groups, namely: bimineralic eclogites, kyanite eclogites and orthopyroxene-bearing eclogites. The classification of all samples and details of their mineralogy are given in Table 1.

Bimineralic eclogites

The bimineralic eclogites contain garnet and clinopyroxene as the primary mineral phases, and account for the majority (34 samples, 76%) of eclogite samples recovered from Rietfontein. In hand specimen, garnets show a variety of colours, from orange, to a darker brown-orange through red to purple. Clinopyroxenes range from light green to a darker emerald green. All samples are relatively homogeneous in terms of mineral distribution and mineral fabric is at best weakly developed.

The samples are on the whole medium to coarse grained. Garnets show a large range in size, from 1 to 15 mm in diameter. Clinopyroxenes tend to be smaller than the garnet grains, varying in diameter from 0.5 to 10 mm. Whereas some samples are equigranular, others show bimodal grain size distribution. Evidence of minor strain occurs in the form of undulose extinction in clinopyroxene, but no strain-induced recrystallization is evident.

Most of the eclogites exhibit alteration to varying degrees, and much of this appears to be a direct result of entrainment within the kimberlite, with minerals such as calcite, serpentine, micas, chlorite and brucite developing as a consequence of this interaction. Fine grained alteration material (mostly mica and amphibole) is common along the grain boundaries and fractures within the mineral grains.

Table 1 Petrographic classification of the Rietfontein eclogites. Modal proportions (vol%) by visual estimation

Classification	Group	Modal mineralogy	Accessory phases (<1%)
Bimineralic eclogites			
JJG105	I	gt 60 cpx 40	Phlogo
PC1		gt 70 cpx 30	
PC3	II	gt 60 cpx 40	Sulphide, phlogo, sp
PC5.2/2	II	gt 40 cpx 60	
PC12	II	gt 30 cpx 70	
Rtfn31.1		gt 45 cpx 55	Sulphide, amph
Rtfn31.2	II	gt 50 cpx 50	
Rtfn31.3	II	gt 45 cpx 55	Rutile; ilmenite
Rtfn43.1	II	gt 60 cpx 40	Rutile; ilmenite
Rtfn43.7		gt 40 cpx 60	Rutile; phlogo
Rtfn43.9	II	gt 40 cpx 60	
Rtfn43.10		gt 45 cpx 55	
Rtfn48.1	II	gt 55 cpx 45	Rutile
Rtfn48.2	I	gt 50 cpx 50	
Rtfn55.1	I	gt 60 cpx 40	
Rtfn55.2	I	gt 80 cpx 20	
Rtfn55.3*		gt 50 cpx 50	
Rtfn55.4	II	gt 30 cpx 70	
Rtfn57.1	II	gt 50 cpx 50	
Rtfn57.2	II	gt 40 cpx 60	
Rtfn57.3	II	gt 50 cpx 50	Sulphide
CMA1	II	gt 30 cpx 70	Amph
CMA2	II	gt 40 cpx 60	Amph
CMA4*		gt 40 cpx 60	
CMA5		gt 50 cpx 50	
CMA7	I	gt 50 cpx 50	Rutile
CMA8	II	gt 50 cpx 50	Amph
CMA9	I	gt 70 cpx 30	Ilmenite
CMA10		gt 50 cpx 50	Rutile; ilmenite
CMA14		gt 40 cpx 60	Rutile
CMA15	II	gt 40 cpx 60	Ilmenite
CMA16		gt 50 cpx 50	
CMA17*	II	gt 70 cpx 30	
CMA18	II	gt 60 cpx 40	
Kyanite eclogites			
JJG2104	II	gt 20 cpx 60 ky 20	
Rtfn54.1	II	gt 60 cpx 30 ky 10	
Rtfn54.2	II	gt 30 cpx 60 ky 10	Rutile
Rtfn54.3	II	gt 45 cpx 45 ky 10	
Rtfn54.4	II	gt 30 cpx 60 ky 10	Rutile; sulphide
Orthopyroxene eclogites			
PC5.2/1		gt 60 cpx 35 opx 5	Sulphide
Rtfn56.1	II	gt 60 cpx 35 opx 5	Phlogo
CMA3	II	gt 30 cpx 50 opx 20	Amph

Table 1 continued

Classification	Group	Modal mineralogy	Accessory phases (<1%)
CMA11		gt 60 cpx 35 opx 5	
CMA12	II	gt 45 cpx 45 opx 10	
CMA13	II	gt 35 cpx 60 opx 5	Rutile

All samples show some evidence of serpentinization of constituent primary phases; accessory phlogopite and amphibole may be secondary

* Although not having modal kyanite, these samples are indistinguishable from the kyanite eclogites on the basis of their garnet and clinopyroxene compositions

Coarser textured secondary minerals also occur in some eclogites and it is often difficult to ascertain if such minerals developed during late stage alteration, or as a consequence of metasomatism in the mantle. These minerals include phlogopite and amphibole (actinolite, edenite and hornblende). Garnet and clinopyroxene occur both as fresh and altered (cloudy) grains, with garnet generally of fresher appearance than clinopyroxene in any given sample. Kelyphite rims around garnets are visible in some samples, and some clinopyroxenes show ‘‘spongy’’ rims. Veins containing rounded vesicles of carbonate material are observable in many samples. Similar veins in other eclogites have been attributed to decompression melting during rapid ascent within the kimberlite (Dawson and Carswell 1990).

Just over half (18 samples, 54%) of the bimineralic eclogites are characterized by relatively straight grain boundaries and unaltered garnets and can be classified as Group II eclogites (MacGregor and Carter 1970). Clinopyroxene in these eclogites commonly have 120° triple junctions. Of the remainder, six samples possess the rounded garnet and interstitial clinopyroxene characteristic of Group I eclogites, while ten samples could not be classified due to excessive alteration. The garnet: clinopyroxene modal proportions range from 30:70 to 80:20, with an average ratio of 50:50. These proportions are however of limited petrologic significance in all but the largest samples, due to the combination of small sample size and coarse grained nature.

One bimineralic eclogite (CMA1) shows the unusual textural feature of garnet exsolution within clinopyroxene. These exsolution lamellae are approximately 0.25 to 0.5 mm in diameter and reach lengths of 1 to 1.5 cm. The garnet lamellae are fresh and up to four or five lamellae can occur in a single, optically continuous clinopyroxene grain. Exsolution of garnet from clinopyroxene in eclogite has been described by Harte and Gurney (1975), Smyth et al. (1989) and Jerde et al. (1993) and is commonly attributed to cooling of a sample from near-solidus conditions to normal mantle lithosphere temperatures (Harte and Gurney 1975; Sautter and Harte 1988). This particular sample also shows fresh, rounded granular garnets, up to 2 mm in diameter, forming an interlocking texture with the clinopyroxene grains.

Accessory minerals in the bimineralic eclogites include sulphides, rutile and ilmenite (Table 1). Most of the eclogites contain at least one accessory mineral. Rutile and ilmenite most commonly take the form of interstitial blebs. Sulphides also occur interstitially, although a few inclusions within garnet were observed. Oxide and sulphide minerals commonly occur in areas of alteration but are inferred to be of primary origin. The sulphides are often heterogeneous, showing distinctly different core and rim compositions, and even different compositions within the core itself. Such zoning and intergrowth of different sulphide minerals may result from the recrystallisation of higher temperature monosulphide solid solutions to a mixture of sulphides at lower temperature.

Kyanite eclogites

Five examples of kyanite eclogite were examined in this study and all can be classified on the basis of texture as Group II eclogites. The samples are all relatively fresh, showing very little sign of alteration relative to the bimineralic and orthopyroxene-bearing eclogites. Garnet, clinopyroxene and kyanite are all equigranular, with an average grain diameter of 1.5–2 mm. Garnets are orange in colour, clinopyroxenes are pale green and kyanite shows a distinctive pale blue colour. The kyanite grains are mostly euhedral, sometimes rounded, and simple twinning is common. Triple junctions among the three phases are common, indicating that the minerals are well equilibrated. Garnet grain shapes are variable, ranging from euhedral, to rounded or irregular, and some contain inclusions of clinopyroxene. Clinopyroxene tends to be irregularly shaped, fractured and shows slight alteration along the rims of the grains, similar to the spongy rims described in the bimineralic eclogites. Serpentinization is common along fractures and both curved and straight grain boundaries occur between the primary minerals. Accessory minerals are scarce, with only interstitial rutile (present in two samples) and sulphide (present in one sample) having been identified. The modal abundance of kyanite in these rocks ranges between 10 and 20 vol%.

Orthopyroxene-bearing eclogites

Six of the Rietfontein eclogites were found to contain orthopyroxene and, although some have textures similar to those characteristic of Group II eclogites, others are difficult to group into MacGregor and Carter’s (1970) classification scheme, due mainly to the degree of alteration. The modal proportion of orthopyroxene in these rocks varies from ~5% to a maximum of 20%. Garnet is consistently the freshest mineral and orthopyroxene the most altered. The eclogites are medium to coarse grained, with garnet grains reaching a maximum diameter of 1 cm. Garnets show a colour range of dark orange to rose pink, whereas clinopyroxenes are dark to emerald green in colour. Subhedral, rounded and irregular garnet and clinopyroxene grain shapes can be observed. Serpentinization is common along fractures and grain boundaries. Triple junctions indicate textural equilibration within the samples and form the basis of the classification as Group II eclogites. Clinopyroxene in some of these orthopyroxene-bearing samples exhibit ''spongy'' rims and decompression melting veins occasionally occur, as described for the bimineralic eclogites. Orthopyroxene in most of the samples is highly altered along fractures and grain boundaries, having been replaced by a dark reddish-brown mineral, similar in appearance to the kelyphite rims often found around garnets, although fresh cores of orthopyroxene still remain in most cases. This high degree of alteration makes it difficult to petrographically distinguish the original grain outlines. Sulphide is present as an interstitial accessory mineral in one sample and rutile in one. Fine grained, pleochroic green amphibole is found rimming the primary mineral grains, and in alteration veins running through the samples.

Mineral chemistry: major elements

The compositions of the major and some accessory minor phases in the Rietfontein eclogites were determined by electron microprobe, and representative analyses are reported in Tables 2, 3, 4, and 5. The full data set of individual analyses is available on request.

Garnet

The garnets are relatively homogeneous, and no systematic zoning, or core-rim variations were observed. Most differences within grains occur in Al_2O_3, FeO, MgO and CaO and are less than 0.5 wt% absolute. These appear to be spatially restricted domains, and are not systematic zoning patterns. There are no differences in major element chemistry between the exsolved garnet lamellae and the granular garnets of sample CMA1, both are Mg-rich (pyrope), with approximately equal proportions of Fe and Ca.

The Rietfontein eclogite garnets are predominantly pyropes (Table 2), but show large variations in Ca–Mg–Fe proportions (Fig. 2a). Only one kyanite eclogite (JJG2104), contains garnet with greater than 50% grossular component. There is a general trend of increasing Ca# (=100 atomic Ca/Ca+Mg+Fe) with decreasing Mg# (= atomic Mg/Mg+Fe), although variation in absolute Fe content is relatively small. The garnets fall into two compositional clusters (Fig. 2a), one of which contains both orthopyroxene-bearing and bimineralic eclogites, while the second, with highest Ca# and lowest Mg#, comprises the kyanite eclogites and a group of three bimineralic eclogites with garnet (and clinopyroxene) compositions essentially identical to those of the kyanite eclogites. These ''high Na, Al'' bimineralic eclogites are interpreted to have equilibrated with kyanite, but lack kyanite in the sample mode due to small size and uneven modal distribution. Although orthopyroxene-bearing eclogite garnets show a range in Mg#, they are comparatively restricted in their CaO content (Table 2).

Minor element concentrations in the pyropes are generally low, with Cr being the most abundant (generally less than 1 wt% Cr_2O_3; Rtfn43.2 has 2.1 wt%). Garnet compositions follow two trends at right angles to one another with respect to Cr versus Ca variation: a high-Cr trend essentially mimics the low-Cr end of the typical lherzolite trend seen in peridotitic garnets from Rietfontein and elsewhere (Gurney 1984), whereas the low-Cr trend, to which ~70% of the garnets belong, is typical of the majority of eclogite garnets from southern African kimberlites (Schulze 1989). Garnets in the kyanite eclogites are uniformly very low in Cr content (<0.1 wt% Cr_2O_3). All garnets are low in Ti content (<0.25 wt% TiO_2) with the higher Ti samples more commonly rutile saturated. Na_2O contents also are very low, with only three samples containing more than 0.09 wt% Na_2O. On this basis, the vast majority of samples fall into the chemical definition of Type II eclogites (McCandless and Gurney 1989), confirming inferences from petrography. One of the high Na garnets is from a bimineralic eclogite (Rtfn53.3), the other is from a high Na–Al eclogite (CMA17).

Clinopyroxene

Representative clinopyroxene compositions are reported in Table 3. Like those in most eclogite xenolith suites, clinopyroxenes from the Rietfontein eclogites show less Ca–Mg–Fe variation than the garnets and plot within a tightly constrained field (Fig. 2a). Clinopyroxenes from the kyanite eclogites have a slightly higher proportion of Ca and a slightly lower proportion of Mg than the bimineralic and orthopyroxene-bearing eclogites, whereas the proportion of Fe in all three groups is similar. The major chemical variation in the Rietfontein clinopyroxenes can be described by the diopside ↔ jadeite substitution. In the IUGS classification scheme (Morimoto 1988), approximately half of the pyroxenes, including all in the kyanite-bearing and ''high-Na, Al'' eclogites are omphacites, and half are

Table 2 Representative analyses of garnets from the Rietfontein eclogites

	Bimineralic eclogites					Kyanite eclogites			Opx-bearing eclogites		
	CMA1 (lamellae)	CMA1 (granular)	CMA2 (core)	PC3 (core)	Rftn57.3 (core)	JJG2104 (core)	Rftn54.4 (rim)	Rftn55.3 (core)	CMA3 (core)	PC5.2/1 (core)	CMA12 (core)
SiO_2	40.63	41.03	40.83	42.12	41.26	39.88	39.13	39.56	40.16	41.39	40.73
TiO_2	0.08	0.07	0.06	0.12	0.10	0.09	0.11	0.25	0.07	0.08	0.13
Al_2O_3	23.21	23.21	23.19	24.52	23.70	22.66	22.71	22.59	22.12	23.45	23.64
Cr_2O_3	0.40	0.40	0.47	0.34	0.64	0.02	0.05	0.02	0.81	0.26	0.18
FeO	11.19	11.28	12.84	7.84	8.85	11.03	14.95	14.76	16.48	13.23	12.82
MnO	0.41	0.43	0.41	0.39	0.36	0.2	0.28	0.27	0.68	0.33	0.39
MgO	14.66	14.62	16.03	20.65	20.45	6.59	9.37	9.66	14.43	17.77	18.12
CaO	9.00	9.12	6.20	4.14	4.47	19.56	13.08	12.72	4.91	3.71	3.84
Na_2O	0.01	0.01	0.01	0.05	0.11	0.06	0.04	0.07	0.01	0.04	0.06
Total	99.58	100.17	100.03	100.16	99.94	100.11	99.71	99.9	99.68	100.25	99.91
Mg#	0.700	0.698	0.690	0.824	0.805	0.516	0.528	0.538	0.609	0.705	0.716

Mg# atomic Mg/(Mg + Fe); all Fe calculated as Fe^{2+}

Table 3 Representative analyses of clinopyroxenes from the Rietfontein eclogites

	Bimineralic eclogites				Kyanite eclogites				Opx-bearing eclogites		
	PC1 (core)	PC3 (core)	Rtfn31.2 (core)	CMA7 (rim)	Rtfn54.1 (core)	Rtfn54.3 (core)	Rtfn54.4 (rim)	CMA17 (rim)	PC5.2/1 (core)	CMA3 (core)	CMA13 (core)
SiO_2	54.70	54.32	54.83	54.21	53.52	53.99	53.57	53.68	55.12	54.2	54.25
TiO_2	0.14	0.28	0.31	0.28	0.28	0.22	0.23	0.46	0.24	0.10	0.11
Al_2O_3	1.54	3.23	5.26	3.39	14.55	12.08	13.27	10.41	5.3	1.66	1.55
Cr_2O_3	0.13	0.31	0.17	0.14	0.03	0.03	0.05	<0.02	0.36	0.35	0.43
FeO	1.86	1.59	3.3	2.65	2.77	1.99	2.38	3.4	3.36	4.21	2.33
MnO	<0.02	0.03	0.02	0.07	0.02	<0.02	0.02	0.03	0.05	0.11	0.06
MgO	17.83	16.6	14.71	16.12	8.43	10.46	9.2	10.17	14.28	16.74	16.9
CaO	23.07	21.37	18.32	20.91	14.28	16.16	14.52	15.6	17.81	21.56	22.68
Na_2O	0.74	1.79	3.28	2.32	5.92	5.16	6.35	5.84	3.64	1.33	1.05
K_2O	<0.02	<0.02	<0.02	<0.02	<0.02	<0.02	<0.02	<0.02	<0.02	<0.02	<0.02
Total	100.04	99.53	100.21	100.09	99.8	100.1	99.61	99.59	100.16	100.26	99.36
Mg#	0.945	0.949	0.888	0.916	0.844	0.904	0.873	0.842	0.883	0.876	0.928

Mg# atomic Mg/(Mg + Fe); all Fe calculated as Fe^{2+}

diopsides. The relatively high proportion of diopsidic clinopyroxenes in the suite implies that, by some definitions, many of these rocks are not strictly speaking eclogites (Carswell 1990).

Figure 2b illustrates the large variation in Na_2O (0.8–6.3 wt%) and MgO content (8.4–17.8 wt%) in clinopyroxenes. A similar range and correlation is exhibited by Al_2O_3 (1.4–14 wt%; Table 3). Two eclogite groups can be identified on the basis of clinopyroxene Na_2O and MgO compositions that correspond essentially to those inferred to have equilibrated with, or without, kyanite. Eclogites with high diopside component in the pyroxene (high Mg, low Na in Fig. 2b) comprise the bimineralic and orthopyroxene-bearing eclogites, and fall within the Group A and lower Group B fields as defined by Taylor and Neal (1989). There is a hint of bimodality in the compositions of this group, as seen in the Ca–Fe–Mg relations of the garnets. The second group comprises the kyanite eclogites, contains low MgO concentrations and high Na_2O concentrations, and also falls within the Group B eclogite field of Taylor and Neal (1989), but closer to the Group B–Group C boundary. This group corresponds precisely with the samples containing high-Ca garnets. FeO within the clinopyroxenes varies between 1.4 and 4.1 wt%, and Cr_2O_3 contents are all below 0.80 wt%. K_2O contents in the Rietfontein eclogites are very low; at or below the detection limit (0.02 wt%) for the analytical procedure used. This reinforces the classification of most of the

Table 4 Representative analyses of orthopyroxenes in the Rietfontein orthopyroxene-bearing eclogites

	PC5.2/1 (Opx)	Rtfn56.1 (Opx)	CMA3 (Opx)	CMA11 (Opx)	CMA12 (Opx)	CMA13 (Opx)
SiO_2	56.80	57.40	56.12	55.72	57.15	57.77
TiO_2	0.04	0.04	0.06	0.06	0.10	0.07
Al_2O_3	0.72	0.79	0.58	0.70	0.70	0.72
Cr_2O_3	0.04	0.05	0.06	0.04	0.01	0.10
FeO	9.33	8.97	12.06	8.80	8.25	7.57
MnO	0.07	0.08	0.20	0.09	0.10	0.11
MgO	32.50	32.27	30.53	33.92	33.22	33.79
CaO	0.32	0.31	0.33	0.28	0.30	0.28
Na_2O	0.13	0.14	0.06	0.12	0.15	0.09
K_2O	0.02	0.03	<.02	0.02	0.03	<0.02
Total	99.94	100.06	100.00	99.74	99.99	100.49
Mg#	0.861	0.865	0.819	0.873	0.878	0.888

Table 5 Representative compositions of accessory phases kyanite, rutile and ilmentite in Rietfontein eclogites

	Kyanite				Rutile				Ilmenite			
	JJG2104	Rtfn54.1	Rtfn54.2	Rtfn54.4	CMA7	Rtfn31.1	Rtfn54.2	Rtfn54.4	CMA10	CMA15	CMA9	Rtfn43.1
SiO_2	37.06	36.63	36.48	36.30	0.04	0.01	0.01	0.00	0.01	0.00	0.01	0.00
TiO_2	0.01	0.01	0.03	0.00	96.74	94.83	96.44	97.64	54.22	48.97	55.81	55.54
Al_2O_3	62.10	62.67	62.22	62.65	0.25	0.08	2.39	0.85	0.46	0.28	0.35	0.28
Cr_2O_3	0.05	0.08	0.08	0.06	0.56	0.45	0.14	0.16	0.50	1.20	0.57	0.33
FeO	0.14	0.20	0.17	0.13	1.92	3.02	0.78	0.57	30.76	40.49	28.67	31.13
MnO	0.02	0.00	0.01	0.00	0.00	0.01	0.00	0.04	0.39	0.37	0.40	0.35
MgO	0.03	0.02	0.02	0.01	0.11	0.64	0.06	0.01	12.45	6.71	13.70	12.30
CaO	0.07	0.00	0.00	0.00	0.13	0.05	0.10	0.00	0.04	0.00	0.02	0.03
Total	99.49	99.60	99.03	99.15	99.75	99.09	99.92	99.28	98.84	98.02	99.53	99.95
FeOc									26.22	31.96	25.39	27.68
Fe_2O_3c									5.05	9.48	3.65	3.83
Total									99.34	98.97	99.90	100.34

Fe_2O_3 calculated following Droop (1987)

Rietfontein eclogites as Group II eclogites according to the scheme of McCandless and Gurney (1989). There is no indication of elevated K_2O in clinopyroxenes coexisting with garnets having higher than average Na_2O contents.

Clinopyroxenes from the orthopyroxene-bearing eclogites do not show any distinct chemical differences to those in the bimineralic and kyanite eclogites, except having slightly higher FeO contents, but overall they show more intra-grain variation than the garnets. One particular sample shows absolute differences of up to 2.5 wt% in CaO and Al_2O_3 in different parts of a grain, but in general, differences are less than 0.5 wt% between the core and rim. Like the garnets, these differences seem to reflect spatially restricted domains, rather than zoning patterns. Late stage effects such as those producing spongy textured rims to the clinopyroxene rims may account for some degree of chemical variation.

Orthopyroxene

Orthopyroxenes within the Rietfontein eclogites are commonly altered around grain boundaries and along fracture zones, but retain pristine areas suitable for analysis. Individual grains are homogeneous, with no compositional zoning and no intra-sample variation. Representative compositions are reported in Table 4. The orthopyroxenes are high-Mg enstatites, with Mg#'s of 0.82–0.89. Al_2O_3 (0.58–0.80 wt%), Cr_2O_3 (<0.10 wt%), TiO_2 (<0.11 wt%), and Na_2O (0.05–0.18 wt%) contents are all low and independent of variation in Mg#. CaO contents are very uniform (0.28–0.33 wt%).

Accessory minerals

Accessory minerals present in the Rietfontein eclogites are kyanite, ilmenite, rutile and sulphides whereas secondary

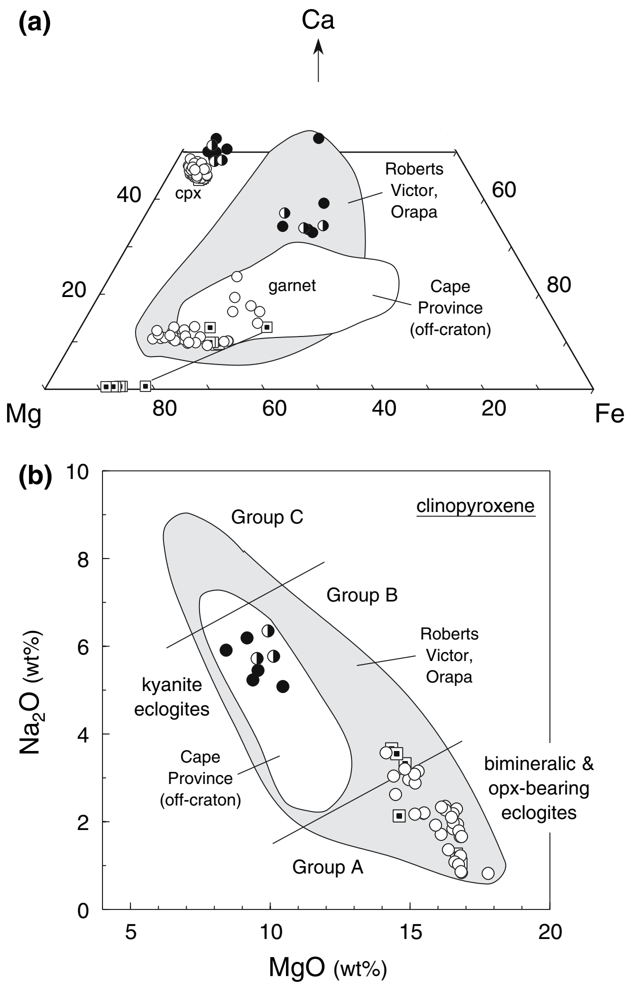

Fig. 2 **a** Compositional variation of clinopyroxene and garnet in Rietfontein eclogites with respect to Ca–Mg–Fe. **b** Na_2O–MgO variation in clinopyroxene from Rietfontein eclogites. Field of on-craton Roberts Victor (Hatton 1978; MacGregor and Manton 1986; McCandless and Gurney 1989; Bell and Rossman 1992) and Orapa (Shee 1978), and off-craton Cape Province (Robey 1981) eclogites are shown for comparison. *Open circles* bimineralic eclogites; *solid circles* kyanite eclogites; *half-filled circles* high Al, Na bimineralic eclogites; *squares* orthopyroxene-bearing eclogites. Group A, B and C subdivisions from Taylor and Neal (1989)

minerals are amphibole and phlogopite. Representative analyses of these minerals are given in Table 5.

Kyanites from the five kyanite eclogites are relatively pure, containing only minor amounts of Fe (0.1–0.2 wt% Fe_2O_3) and Cr (0.05–0.1 wt% Cr_2O_3).

Rutile was analyzed in 11 samples and shows significant ranges in the minor components Al_2O_3 (0.1–2.4 wt%), Cr_2O_3 (0.1–2.6 wt%), FeO_T (0.8–4.9 wt%) and MgO (<0.03 – 0.83 wt%). In addition, there is gross intra-sample and intra-grain heterogeneity in all minor elements except Cr.

Ilmenites generally exhibit high MgO (11.7–13.9 wt%) contents, typical of upper-mantle derived ilmenites (Haggerty 1991), although ilmenites in one sample (CMA15) have lower, more moderate MgO (~6 wt%) contents. This latter composition is similar to that of ilmenite from eclogites at Kaalvallei and Orapa (Viljoen 1994; Shee 1978; Tollo 1982). All ilmenites are notably poor in Cr compared with those in peridotites, but are within the range found in some megacryst suites.

Sulphides are commonly altered and the degree of alteration and exsolution made representative analyses difficult to obtain. However, it was possible to determine that the sulphides were not homogeneous, as many showed visibly different cores and rims. It was also noted that the sulphides showed significant chemical variation within the cores, so the grains are entirely heterogeneous. Variable proportions of Fe, Cu and Ni were measured in the sulphides and minor amounts of Zn (0–0.3 wt%) and Co (0.1–1.4 wt%) were also noted.

Amphiboles in the Rietfontein eclogites span a range of compositions and are classified variably as hornblende, actinolite and edenite. Significant intra-sample compositional heterogeneity exists, reflecting their unequilibrated, secondary origin. The samples are relatively magnesian, with Mg# in the range 0.72–0.90. In the hornblende–edenite series, Al_2O_3 contents range from 9.5–17.7 wt%, and Na_2O contents from 3.5 to 4.5 wt%. Most samples contain appreciable K_2O, up to 1.2 wt%. TiO_2 contents are low (0.1 – 0.6 wt%).

The *mica* identified in the Rietfontein eclogites is phlogopite, with MgO contents of 20–24 wt% and K_2O contents of 8.3–9.4 wt%.

Mineral chemistry: trace elements

A range of trace elements were determined in co-existing garnet and clinopyroxene in four kyanite eclogites, twelve bimineralic eclogites and three orthopyroxene-bearing eclogites, and analyses are reported in Table 6. In general Sc, Zr and Sr concentrations in the garnets are all highly variable (17.2–157, 2.2–24 and 0.079–3.5 ppm, respectively), whereas Ni and Y concentrations are somewhat less variable (14–41 and 8.3–27 ppm, respectively). Garnets from the kyanite eclogites and high Na, Al eclogites (hereafter simply referred to as kyanite eclogites) are markedly different in their trace element abundances compared to the bimineralic and orthopyroxene-bearing eclogites, with the former having higher Sr and middle REE contents than the latter two varieties (Table 6); they also have Sc and Zr abundances that overlap only at the low end of the range of the latter two groups.

Rare earth element patterns of the garnets are all strongly LREE depleted when normalised to chondrites, decreasing smoothly from constant HREE normalised abundances of 5–20 × chondrite to <0.2 × chondrite in the LREE (Fig. 3a). Garnets in the kyanite eclogites are distinguished by their slightly less depleted LREE abundances, their raised Nd, Sm and Eu abundances, and their significant positive Eu anomalies (Eu/Eu* = 1.4–2.3). Moderate positive Eu anomalies (Eu/Eu* = 1.2–1.9) occur also in six of the bimineralic eclogites (PC1, JJG105, Rtfn31.1, Rtfn43.1, CMA4, CMA17). The exsolved garnet lamellae in CMA1 have REE patterns indistinguishable from other bimineralic eclogites. When normalised to primitive mantle abundances, the trace element patterns of garnets in the kyanite eclogites are again clearly distinct from those of the other two groups (Fig. 3b). In addition to having raised light to middle REE abundances, the kyanite eclogite garnets do not show the characteristic relative depletion in Sr compared to adjacent elements of similar incompatibility, and are strongly depleted in Zr and Ti, resulting in substantial negative Zr and Ti anomalies (Fig. 3b). Garnets in the bimineralic and orthopyroxene-bearing eclogites have similar primitive mantle normalized trace element patterns, both having distinct negative Sr anomalies and subdued negative Ti anomalies. Garnets in some samples from both groups also show a distinct relative depletion in Zr (although much less marked than that in the kyanite eclogites; Fig. 3b).

The Rietfontein eclogite clinopyroxenes have highly variable Sr (26–417 ppm), Sc (4.5–47.7 ppm) and Zr (2.3–44.7 ppm), and less variable Ni (149–508 ppm; Table 6). Chondrite normalised REE patterns for selected clinopyroxenes are illustrated in Fig. 4a. Clinopyroxenes in the bimineralic and orthopyroxene-bearing eclogites exhibit uniformly LREE enriched trends with variable La/Yb$_n$ ratios and LREE being enriched by 5–100 × chondrite and HREE 0.3–1 × chondrite. A couple of samples (CMA14, Rtfn31.1) have clinopyroxene perhaps showing a small positive Eu anomaly (Eu/Eu* = 1.15–1.17). The chondrite normalised REE patterns of clinopyroxenes from the kyanite eclogites are markedly different to those in the bimineralic and orthopyroxene-bearing eclogites. They show enrichment in the middle REE and strong depletion in LREE, giving a ‘‘humped’’ pattern (Fig. 4a); HREE (and Y) abundances are also lower (0.1–0.2 × chondrite) than in the other two groups.

The trace element difference between clinopyroxenes in the kyanite eclogites and those in the bimineralic and orthopyroxene-bearing eclogites is even more marked when one considers primitive mantle normalised abundance patterns (Fig. 4b). Whereas there is a general increase in abundance in more highly incompatible elements, there are distinct relative depletions (negative anomalies) in Ti, Zr and Nb in clinopyroxene in the bimineralic and orthopyroxene-bearing eclogites. In contrast, in addition to the differences in REE patterns, clinopyroxenes in the kyanite eclogites have no Ti or Zr anomalies, Nb is similar to La, and they show a strong positive Sr anomaly (Fig. 4b). It is noteworthy that the absence of relative depletion in Zr and Ti in the kyanite eclogite clinopyroxenes contrasts with their coexisting garnets, which have very strong negative anomalies in these two elements (compare Figs. 3b, 4b).

Mineral chemistry: oxygen isotopes

Garnets from five eclogites (two kyanite, three bimineralic) were selected for oxygen isotope analysis, and results are presented in Table 7. Samples were selected on the basis of the size and freshness of their constituent garnets. Garnet separates from samples JJG2104, CMA4 and CMA14 were analysed in duplicate to assess precision, which was found to be good for samples CMA4 and CMA14 (within 0.3‰), but less satisfactory for sample JJG2104 (~0.9‰ difference). The latter sample contained the freshest garnet grains and the large difference is thus though to reflect analytical uncertainty, rather than alteration.

The most Ca-rich sample (JJG2104) exhibits the highest δ^{18}O values, 6.84 and 5.95‰ (av. = 6.40‰), although the reproducibility for this sample was clearly poor. There is a broad negative correlation between δ^{18}O and SiO_2 and MgO, and positive correlation with FeO, with the most Mg-rich samples, Rt43.2 and Rt55.1, containing garnets with the lowest δ^{18}O values, 5.24 and 5.16‰, respectively. The Rietfontein eclogite garnets all fall within, or very close to, the normal mantle range of 5.5 ± 0.7‰ (Mattey et al. 1994).

Whole rock chemistry

Whole-rock compositions of the Rietfontein eclogites have been reconstructed using the analysed compositions of the primary minerals and their modal proportions. Due to the small size of many of the xenoliths relative to the size of the mineral grains, the range in modal abundances (cpx:gt = 20:80 to 70:30) is unlikely to reflect that of the original bulk protolith. Consequently, a single ratio of 50:50 (the overall average) has been used for the bimineralic eclogites, and 0.44:0.44:0.12 (cpx:gt:opx) for the orthopyroxene-bearing eclogites. The major element compositions of the kyanite eclogites were calculated using a fixed abundance of 10% kyanite. However, it should be noted that trace element abundances were not measured in kyanite, and so its presence served only as a dilution effect. Although rutile occurs in some samples, its relative abundance when present is very low, and difficult to extrapolate to the original protolith. Rutile has therefore not been

Table 6 Trace element analyses in garnet and clinopyroxene in Rietfontein eclogites

	Kyanite eclogites					Bimineralic eclogites												Orthopyroxene-bearing eclogites		
	JJG 2104	Rtfn 54.1	Rtfn 54.4	CMA 4	CMA 17	JJG 105	PC 1	CMA 1	CMA 5	CMA 8	CMA 14	Rtfn 31.1	Rtfn 43.1	Rtfn 48.2	Rtfn 55.1	Rtfn 55.2	Rtfn 57.1	PC 5.2/1	CMA 3	CMA 12
Sc	17.2	27.9	39.3	32.5	53.8	47.1	32.2	157	51.4	89.8	66.8	51.3	77.5	79.4	65.3	53.4	48.7	48.5	145	53.5
Ni	28.1	30.1	19.8	39.5	14.2	25.5	26.8	24.3	24.7	23.1	24.0	22.4	17.4	24.4	23.4	25.4	24.7	40.8	21.2	21.2
Sr	1.49	2.10	1.98	3.51	1.62	0.16	0.82	0.65	0.33	0.46	0.15	0.12	0.097	0.099	0.17	0.079	0.12	0.12	0.67	0.12
Y	8.26	16.0	21.4	13.1	17.1	10.2	9.23	18.2	24.2	11.8	17.2	9.60	20.8	6.70	19.7	7.37	10.6	11.6	17.2	26.9
Zr	2.24	6.147	6.64	5.65	5.95	4.71	3.48	3.37	11.2	19.9	4.48	5.84	21.8	20.2	23.5	11.0	4.48	4.26	6.83	10.1
La	ND	ND	ND	0.003	0.034	0.014	ND	0.009	0.011	0.020	0.008	0.009	0.006	0.016	0.006	ND	0.003	0.007	ND	ND
Ce	0.072	0.12	0.14	0.083	0.32	0.070	0.071	0.046	0.071	0.13	0.047	0.053	0.075	0.11	0.11	0.033	0.064	0.037	0.028	0.063
Nd	1.27	3.40	2.75	2.67	1.49	0.15	0.71	0.14	0.25	0.53	0.31	0.25	0.33	0.48	0.43	0.47	0.35	0.21	0.13	0.38
Sm	0.92	3.24	2.55	1.70	1.40	0.24	0.58	0.28	0.45	0.67	0.42	0.44	0.42	0.53	0.39	0.72	0.29	0.44	0.17	0.52
Eu	0.80	1.62	1.37	0.91	0.73	0.19	0.50	0.18	0.29	0.36	0.26	0.24	0.30	0.21	0.18	0.24	0.19	0.25	0.12	0.31
Gd	1.26	3.28	3.33	1.87	2.44	0.77	1.02	1.26	1.83	1.52	1.29	0.86	1.43	0.94	1.16	0.84	0.95	1.02	0.69	2.05
Dy	1.40	3.20	4.14	2.26	3.14	1.58	1.49	3.00	3.91	1.89	2.58	1.46	2.93	1.12	2.85	1.17	1.79	1.70	2.32	4.08
Er	0.95	1.54	2.30	1.51	1.84	1.15	1.05	2.09	2.79	1.28	2.24	1.06	2.39	0.65	2.50	0.91	1.27	1.29	2.32	2.88
Yb	0.84	1.23	1.94	1.98	1.97	1.23	1.04	1.83	3.19	1.18	2.33	1.10	2.68	0.78	2.78	0.86	1.23	1.40	2.57	3.56
Cpx	JJG 2104	Rtfn 54.1	Rtfn 54.4	CMA 4	CMA 17	JJG105	PC 1	CMA 1	CMA 5	CMA 8	CMA 14	Rtfn 31.1	Rtfn 43.1	Rtfn 48.2	Rtfn 55.1	Rtfn 55.2	Rtfn 57.1	PC 5.2/1	CMA 3	CMA 12
Sc	4.57	6.32	9.76	7.13	17.7	19.4	15.5	41.3	20.5	23.0	24.9	20.6	26.1	24.4	22.3	16.7	18.9	16.4	47.7	22.0
Ni	419	294	226	449	179	340	149	442	299	327	292	350	213	324	281	313	370	508	382	293
Sr	138	288	372	185	107	300	168	26.0	166	215	210	178	327	417	215	221	241	328	33.6	241
Y	0.074	0.26	0.38	0.24	0.37	2.65	2.77	0.62	3.98	5.16	1.19	1.39	3.72	2.16	3.03	0.98	2.33	1.70	1.17	3.82
Zr	3.30	8.56	11.6	7.57	6.73	31.8	9.84	2.25	36.2	43.9	7.18	11.5	43.9	44.7	42.9	19.6	24.3	18.3	6.30	32.7
Nb	0.44	0.36	ND	ND	0.03	2.41	0.53	0.011	0.23	2.22	0.086	0.11	0.87	ND	0.56	0.19	1.00	0.75	0.37	0.091
Th	ND	ND	ND	ND	0.11	0.49	0.26	0.059	0.42	0.82	0.36	0.15	1.08	ND	0.84	0.65	0.26	0.49	0.15	0.45
La	0.008	0.026	0.069	0.003	1.30	12.1	4.09	1.13	6.85	10.9	4.45	3.01	19.9	25.3	11.0	6.96	9.54	9.03	1.60	11.2
Ce	0.184	0.52	0.93	0.10	3.92	32.2	9.02	2.48	18.3	26.9	8.02	9.22	45.5	62.7	25.9	19.8	26.4	20.3	3.33	28.3
Nd	0.72	2.68	3.28	2.13	2.67	17.6	9.28	1.24	12.2	16.2	5.02	6.74	21.6	28.0	13.9	17.4	14.8	11.6	2.02	13.9
Sm	0.22	0.68	0.73	0.56	0.62	3.09	2.71	0.40	3.01	3.92	1.26	1.57	3.76	4.00	2.67	3.37	2.82	2.37	0.55	3.06
Eu	0.078	0.24	0.27	0.16	0.17	0.91	0.68	0.11	0.93	1.18	0.39	0.50	1.09	1.06	0.76	0.62	0.78	0.68	0.13	0.93
Gd	0.068	0.39	0.29	0.26	0.36	2.11	1.97	0.41	2.65	3.34	0.84	1.11	2.33	2.30	1.83	1.18	1.77	1.49	0.50	2.48
Dy	0.041	0.065	0.13	0.063	0.13	0.83	0.83	0.24	1.30	1.64	0.37	0.50	1.16	0.77	0.98	0.38	0.69	0.60	0.35	1.27
Er	0.053	0.036	0.038	0.032	0.025	0.20	0.21	0.062	0.29	0.43	0.112	0.10	0.28	0.20	0.25	0.087	0.15	0.11	0.12	0.23
Yb	0.021	0.041	0.017	0.031	0.017	0.10	0.050	0.21	0.21	0.027	0.15	0.074	0.13	0.069	0.090	0.058	0.048	0.045	0.041	0.13

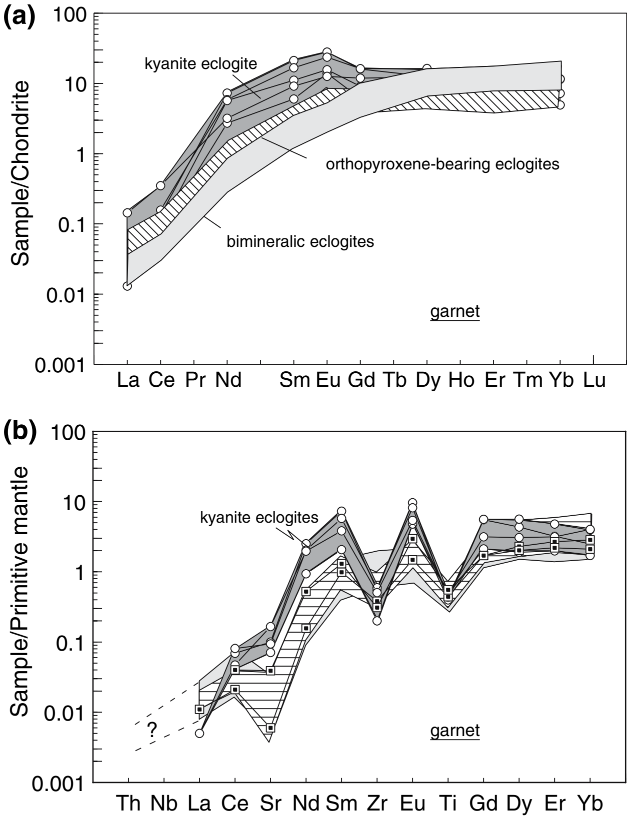

Fig. 3 **a** Chondrite normalized rare earth element patterns in garnets, and **b** primitive mantle normalized trace element abundances in garnet in Rietfontein eclogites. Not all samples are shown to aid clarity. Normalising values from Sun and McDonough (1989)

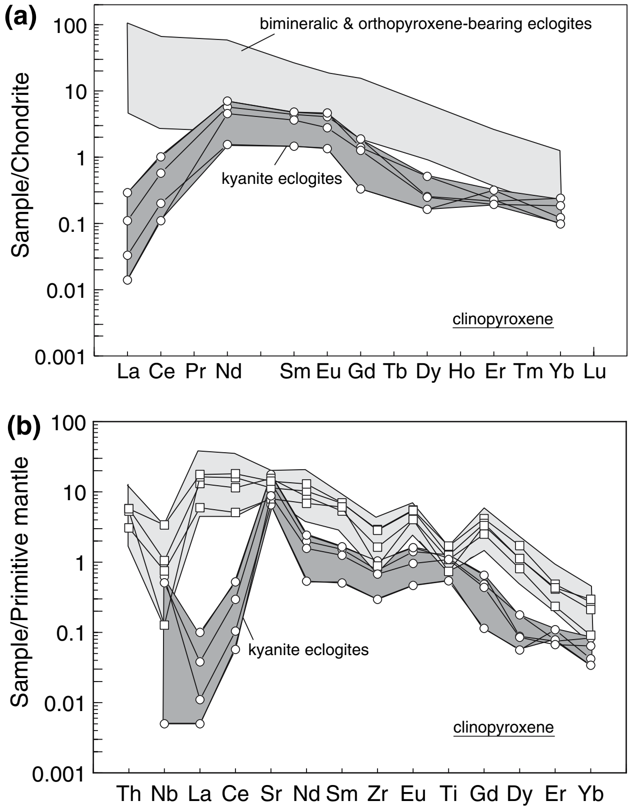

Fig. 4 **a** Chondrite normalized rare earth element patterns in clinopyroxene, and **b** primitive mantle normalized trace element abundances in clinopyroxene in Rietfontein eclogites. Not all samples are shown to aid clarity. Normalising values from Sun and McDonough (1989)

included in any of the reconstructed compositions; however, its presence would obviously strongly affect Ti and Nb abundances and influences certain interpretations, as discussed later.

Table 8 presents reconstructed bulk-rock major and trace element compositions of the Rietfontein eclogites, and selected compositional variations are depicted in Figs. 5, 6 and 7. The bulk composition of the kyanite eclogites is clearly distinct from that of the orthopyroxene-bearing and bimineralic eclogites, with the former being poorer in MgO (~7–10 wt%) and SiO_2 (~45–47 wt%) and richer in Al_2O_3 (~16–23 wt%) and Na_2O (~2–3 wt%); the bimineralic and orthopyroxene-bearing eclogites have 15.3–18.8 wt% MgO, 47.1–49.0 wt% SiO_2, 9.6–14.2 wt% Al_2O_3 and 0.8–1.7 wt% Na_2O. In contrast, CaO contents of the kyanite eclogites (12–16 wt%) overlap with those shown by the bimineralic and orthopyroxene-bearing eclogites (Fig. 5). TiO_2 contents are low (<0.4 wt%) in all the eclogites, although this could in part reflect that accessory rutile, present in some samples and absent in others, was not included in the bulk rock calculations. FeO contents of the kyanite eclogites (6–10 wt%) overlap the range shown by the orthopyroxene-bearing and bimineralic eclogites, although the most MgO-rich bimineralic eclogites extent to unusually low FeO contents (<5 wt%). The Mg# of the kyanite eclogites (Mg# = atomic Mg/Mg+Fe, with Fe_2O_3/FeO set to 0.15) is less than 0.74, whereas the bimineralic and orthopyroxene-bearing eclogites have Mg# > 0.76 (extending to ~0.90). In terms of major elements there is little to distinguish between the orthopyroxene-bearing and bimineralic eclogites (Fig. 5; Table 8). The bulk-rock compositional characteristics reflect the

Table 7 $\delta^{18}O$ values (‰) for selected garnets from the Rietfontein eclogites

Sample	$\delta^{18}O$
JJG2104	6.84
	5.95
CMA4	5.58
	5.82
CMA14	5.99
	5.61
Rtfn43.2	5.24
Rtfn55.1	5.16

Table 8 Reconstructed bulk rock major and trace element compositions of Rietfontein eclogites

	Kyanite eclogites					Opx-bearing eclogites			Bimineralic eclogites											
	JJG2104	Rtfn 54.1	Rtfn 54.4	CMA4	CMA17	PC 5.2/1	CMA3	CMA12	JJG 105	PC1	Rtfn 31.1	Rtfn 43.1	Rtfn 48.2	Rtfn 55.1	Rtfn 55.2	Rtfn 57.1	CMA1	CMA5	CMA8	CMA14
SiO_2	44.92	45.46	45.07	46.74	46.24	49.01	48.24	48.79	47.62	48.30	47.19	47.65	47.65	48.53	48.55	47.95	47.08	47.27	47.59	46.89
TiO_2	0.07	0.16	1.13	0.18	0.37	0.15	0.08	0.23	0.22	0.15	1.14	1.03	0.12	0.20	0.19	0.18	0.10	0.26	0.12	1.12
Al_2O_3	26.71	22.94	22.25	17.82	16.36	13.04	9.64	13.05	14.20	13.04	13.53	13.15	13.77	13.46	13.53	13.74	12.92	13.90	12.81	13.38
Cr_2O_3	0.02	0.03	0.06	0.28	0.03	0.28	0.48	0.18	0.31	0.17	0.24	0.28	0.86	0.35	0.41	0.20	0.31	0.19	0.91	0.05
FeO	5.34	7.95	7.72	7.13	9.59	8.35	10.49	8.03	8.74	5.36	8.72	6.22	4.59	4.99	4.44	8.75	6.77	7.00	6.21	9.24
MnO	0.08	0.12	0.12	0.13	0.17	0.18	0.32	0.20	0.19	0.17	0.20	0.21	0.23	0.22	0.17	0.18	0.24	0.18	0.33	0.20
MgO	6.29	7.66	8.31	9.95	9.27	17.71	18.19	17.94	16.05	18.79	16.21	17.68	18.64	17.93	18.32	15.99	15.33	16.94	17.29	14.68
CaO	14.24	12.88	12.07	14.80	14.14	9.70	10.77	9.98	11.38	13.84	11.41	12.41	12.43	12.63	12.99	11.44	15.80	11.26	13.36	13.32
Na_2O	2.11	2.64	2.79	2.87	2.92	1.68	0.53	1.62	1.50	0.43	1.49	1.00	1.03	0.92	0.84	1.30	0.67	1.59	1.12	1.12
K_2O	0.00	0.00	0.00	0.01	0.00	0.01	0.00	0.01	0.01	0.00	0.00	0.00	0.00	0.00	0.00	0.00	0.00	0.00	0.00	0.00
Total	99.79	99.84	99.52	99.91	99.08	100.11	98.73	100.02	100.22	100.26	100.14	99.63	99.33	99.23	99.44	99.75	99.22	98.58	99.75	99.99
Mg#	0.704	0.661	0.685	0.738	0.661	0.811	0.778	0.819	0.788	0.876	0.790	0.852	0.891	0.879	0.893	0.787	0.821	0.830	0.849	0.763
Sc	10.9	17.1	24.5	19.8	35.8	32.4	96.2	37.8	32.5	23.9	35.9	51.8	51.9	43.8	35.0	33.9	98.9	35.9	56.4	45.9
Ni	223	162	123	244	96.7	274	202	157	186	87.9	186	115	174	152	169	189	233	162	175	158
Sr	69.6	145	187	94.4	54.1	164	17.2	120	194	84.3	89.2	163	209	107	111	104	13.3	83.2	108	105
Y	4.17	8.11	10.9	6.68	8.75	6.63	9.17	15.3	6.62	6.00	5.50	12.2	4.43	11.3	4.17	6.05	9.42	14.1	8.49	9.22
Zr	2.77	7.35	9.12	6.61	6.34	11.3	6.56	21.4	23.7	6.66	8.67	32.8	32.5	33.2	15.3	9.27	2.81	23.7	31.9	5.83
Nb	0.22	0.18	ND	0.002	0.015	0.37	0.18	0.045	1.20	0.27	0.056	0.43	ND	0.28	0.094	0.50	0.006	0.11	1.11	0.043
Th	ND	ND	ND	ND	0.053	0.25	0.075	0.23	0.24	0.13	0.075	0.54	ND	0.42	0.32	0.13	0.030	0.21	0.41	0.18
La	ND	0.007	0.027	0.003	0.67	4.52	0.80	5.61	7.86	2.04	1.51	9.97	12.6	5.52	3.48	3.90	0.57	3.43	5.47	2.23
Ce	0.13	0.32	0.54	0.092	2.12	10.2	1.68	14.2	21.5	4.54	4.64	22.8	31.4	13.0	9.94	9.65	1.26	9.18	13.5	4.03
Nd	1.00	3.04	3.01	2.40	2.08	5.90	1.07	7.13	11.4	4.99	3.50	11.0	14.3	7.17	8.96	5.13	0.69	6.25	8.34	2.67
Sm	0.57	1.96	1.64	1.13	1.01	1.40	0.36	1.79	2.03	1.64	1.00	2.09	2.27	1.53	2.04	1.09	0.34	1.73	2.29	0.84
Eu	0.44	0.93	0.82	0.53	0.45	0.46	0.12	0.62	0.63	0.59	0.37	0.70	0.64	0.47	0.43	0.36	0.15	0.61	0.77	0.33
Gd	0.66	1.83	1.81	1.07	1.40	1.25	0.60	2.26	1.62	1.49	0.98	1.88	1.62	1.49	1.01	1.04	0.84	2.24	2.43	1.07
Dy	0.72	1.63	2.14	1.16	1.64	1.15	1.33	2.67	1.29	1.16	0.98	2.04	0.94	1.91	0.78	1.13	1.62	2.60	1.76	1.48
Er	0.50	0.79	1.17	0.77	0.93	0.70	1.22	1.56	0.68	0.63	0.58	1.33	0.42	1.38	0.50	0.69	1.07	1.54	0.86	1.17
Yb	0.43	0.63	0.98	1.01	0.99	0.72	1.30	1.84	0.69	0.59	0.59	1.40	0.42	1.44	0.46	0.64	0.94	1.70	0.70	1.18

Mg# calculated assuming $Fe_2O_3/FeO = 0.15$. See text for further discussion

Fig. 5 Variations of reconstituted bulk rock compositions of Rietfontein eclogites. Fields for MORB (le Roex et al. 1983, 1985; le Roux et al. 2002), Archean komatiites and picrites (*dark grey*), Archean basalts (*dashed outline*) and oceanic gabbros and pyroxenites (*intermediate grey*) from Barth et al. (2001, 2002b). Field for boninites from Bloomer (1989), Brown and Jenner (1989), Coish (1989) and Kerrich et al. (1998). Symbols as in Fig. 2

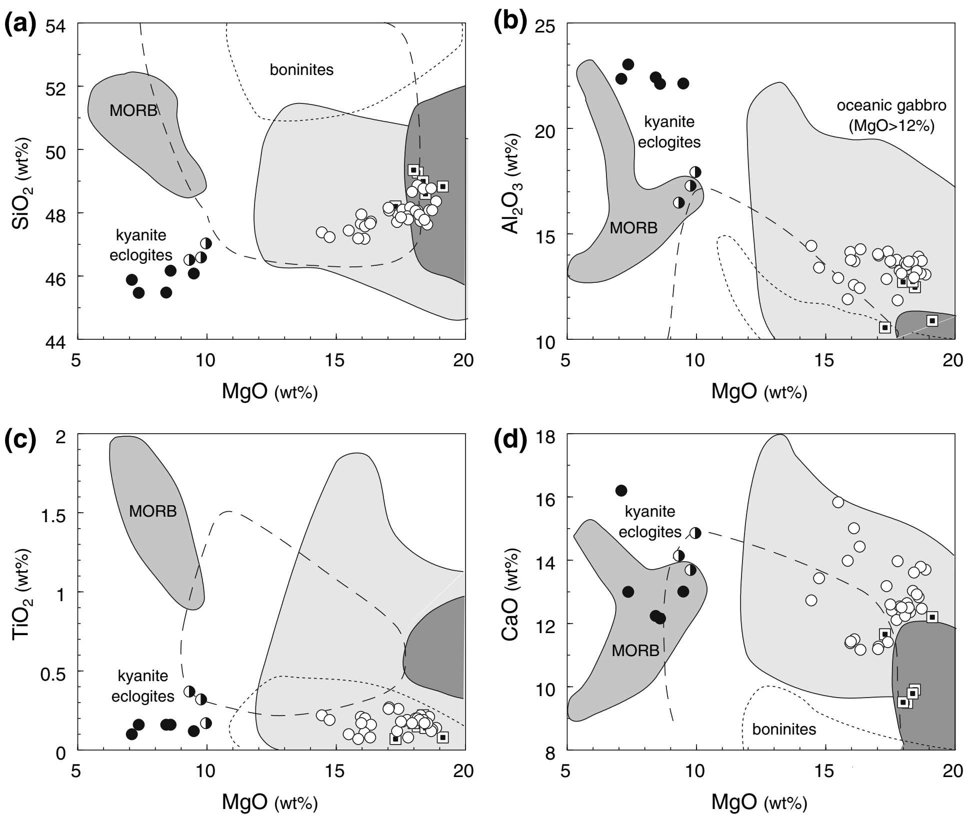

overall basaltic nature of the kyanite eclogites, in contrast to the more picritic nature of the bimineralic and orthopyroxene-bearing eclogites, with their higher MgO (~14–19 wt%) and lower Al_2O_3 (~10–15 wt%) and Na_2O (<1.9 wt%) contents (Table 8).

Trace element compositions serve to further distinguish between the three groups of eclogites. Table 8 shows that, although absolute trace element abundances are quite variable, e.g. Ni (88–274 ppm), Sr (~50–200 ppm; except CMA1, 3), Sc (10–55 ppm; CMA1, 3 excepted) and La < 0.01 to 12 ppm, and elements such as Zr (3–33 ppm) and Y (4–14 ppm) are particularly low for typical mafic magmas, the kyanite eclogites tend to have consistently lower bulk rock abundances of the high field strength elements (Table 6; Fig. 7). Figure 6 shows chondrite normalised REE abundances of the calculated bulk rock compositions, and it is clear that whereas the kyanite eclogites are strongly LREE depleted (LREE <0.3 × and HREE 2–6 × chondrite; $La/Yb_n<0.05$), the orthopyroxene-bearing eclogites have flat chondrite normalised REE patterns (Fig. 6a). In contrast, the bimineralic eclogites show two groups of patterns (Fig. 6b)—one slightly LREE enriched ($La/Yb_n = 5–21$), the other flat to LREE depleted ($La/Yb_n = <1$). The kyanite eclogites are further characterised by having strong positive Eu anomalies (Eu/Eu* = 1.5–2.2), which are absent in the other eclogite groups. All three groups have remarkably flat HREE abundances (3–10 × chondrite).

Primitive mantle normalised patterns of the calculated bulk rock compositions are similarly informative (Fig. 7). In addition to their strong depletion in LREE, the kyanite eclogites have marked negative anomalies (relative depletion) in Ti and Zr, and enrichment in Sr. Nb is more variable and perhaps slightly enriched relative to La, but would be strongly influenced by the presence of rutile, which as discussed earlier has not been included in the calculations. The bimineralic and orthopyroxene-bearing eclogites show a similar depletion in Ti, but only the bimineralic eclogites show a significant relative depletion in Zr. Both groups show strong relative depletion in Nb (La/Nb > 2.5). Addition of as little as 0.1% rutile to the mode is sufficient to remove the negative Ti anomaly, and providing the rutile has on the order of 500 ppm Nb (Barth et al. 2001 quote values 70–1,700 ppm) would negate the negative Nb anomaly seen in the bimineralic eclogites, and many would have a slight positive Nb anomaly. Whereas the relative depletion in Ti and Nb could be a consequence of the omission of rutile in calculating the bulk rock compositions, this is unlikely to be the cause of the negative Zr anomaly.

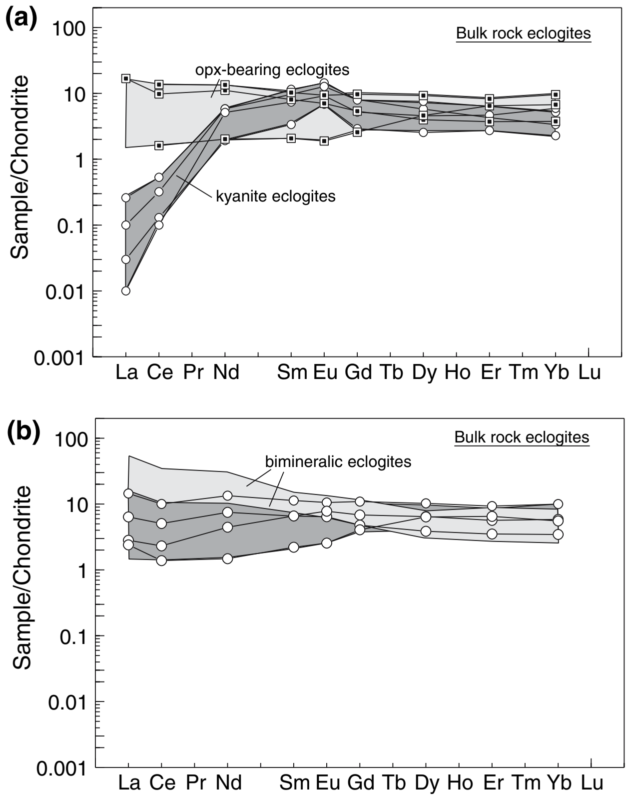

Fig. 6 Chondrite normalized REE patterns for reconstituted bulk rock compositions of Rietfontein eclogites. **a** Kyanite and orthopyroxene-bearing eclogites, **b** bimineralic eclogites. Normalising values from Sun and McDonough (1989)

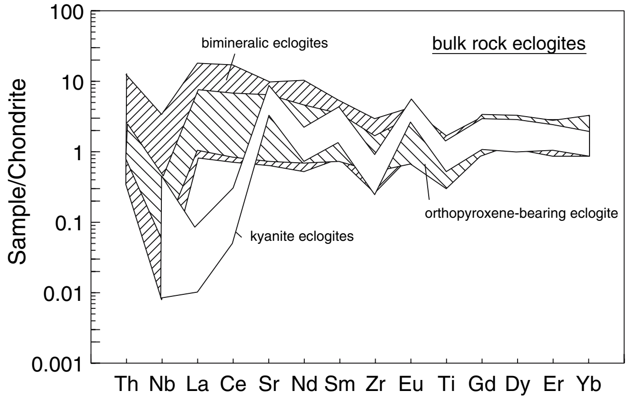

Fig. 7 Primitive mantle normalized trace element patterns for reconstituted bulk rock compositions of Rietfontein eclogites. Normalising values from Sun and McDonough (1989)

Thermobarometry

Methods

Few mineral thermobarometers are applicable to the mineralogically restricted assemblages characteristic of the Rietfontein eclogites and most kimberlite-derived eclogite suites. For the majority of samples, garnet-clinopyroxene thermometry at an assumed pressure (20, 30 and 40 kbar) was the only applicable method (Table 9). For the six orthopyroxene-bearing samples, Al-in-opx barometry may be combined with either Fe-Mg exchange thermometry (gt-cpx or gt–opx) or pyroxene solvus equilibria. We used the Al-in-opx barometer calibrations of Brey and Köhler (1990) $[P_{BK}]$ and Taylor (1998) $[P_{Ta}]$, combined with the gt-opx Fe–Mg exchange thermometer of Harley (1984) $[T_{Ha}]$, the gt-cpx Fe–Mg exchange thermometers of Ellis and Green (1979) $[T_{EG}]$, Krogh (1988) $[T_{Kr}]$ and Berman et al. (1995) $[T_{Be}]$ and the pyroxene solvus thermometers of Wells (1977) $[T_{We}]$, Taylor (1998) $[T_{Ta}]$ and Brey and Köhler (1990) $[T_{BKN}, T_{Ca\text{-}in\text{-}opx}]$. Selected results for the opx-bearing eclogites are given in Table 10.

Temperature estimates

Two first order observations from the data presented in Tables 9 and 10 are that the temperatures are relatively low for eclogite suites in kimberlites, not exceeding 1,050°C for any sample or method of calculation and that the different methods give considerably different results.

Garnet-clinopyroxene exchange thermometry is the method applicable to the greatest number of samples. Results from the three calibrations of this thermometer, T_{EG}, T_{Kr} and T_{Be}, have significant differences among one another that are strongly correlated with Ca in garnet. The T_{EG} calibration produces the smallest T range (~200°C) and is the only calibration that produces no consistent composition-correlated temperature variation. Results for T_{Kr} are similar to T_{EG} at high Ca in garnet, but are consistently 100° lower at low Ca in garnet. In contrast, T_{Be} produces the opposite deviation, with high-Ca garnets (kyanite eclogites) recording temperatures lower by up to 300°C. Many of the garnets in these rocks have extremely low Ca contents (<4 wt%), even lower than most peridotitic garnets, and accurate calibration of the Ca-dependence of K_d is important. On face value, T_{EG} is therefore preferred among the gt-cpx thermometers.

The range of T_{EG} is 815–1,012°C, with a mean of 908 ± 50°C (1σ). Kyanite eclogites record a range at the high P–T end (891–1,012°C, mean 939 ± 38°C) compared with orthopyroxene-bearing eclogites, which record lower than average P–T (824–968°C, mean 886 ± 55°C). Statistics for the bimineralic eclogites (815–993°C, mean 904 ± 50°C) are similar to those of the overall population, reflecting the likelihood, discussed above, that the bimineralic samples really contain representatives of all groups.

The unknown concentrations of Fe^{3+} in clinopyroxene, in particular the potential for systematic variations in Fe^{3+} correlated with petrologic type and errors in calculating Fe^{3+}, introduce uncertainty into the accuracy of these

Table 9 Temperatures calculated for eclogites at assumed pressures of 2, 3 and 4 GPa using thermometers of Ellis and Green (1979) (EG), Krogh 1988 (Kr) and Berman et al. (1995) (Be)

Sample	EG 2 GPa cores	EG 2 GPa rims	EG 3 GPa	Kr 3 GPa	Be 3 GPa	EG 4 GPa
Kyanite eclogites						
JJG2104	928		957	860	664	983
Rftn54-1	962		1012	1000	711	1043
Rftn54-2	859	855	891	871	638	920
Rftn54-3	874	872	906	887	647	935
Rftn54-4	868	880	905	887	635	934
Rftn55-3	917	919	947	935	682	978
CMA17	920	913	947	934	704	977
CMA4	912	913	944	924	660	973
Orthopyroxene-bearing eclogites						
PC5.2/1	881		917	805	862	953
Rftn56-1	854		886	774	836	920
CMA3	792		824	735	818	856
CMA11	862		897	791	848	932
CMA12	923	936	968	866	922	1004
CMA13	856		825	735	796	857
Bimineralic eclogites						
CMA5	899		931	825	889	967
CMA6	803		841	756	813	873
CMA7	916	936	957	858	937	993
CMA8	967		990	929	970	1026
CMA9	897	894	931	855	899	965
CMA10	884		920	826	929	955
CMA16	920		988	889	892	1026
CMA18	954		993	909	925	1030
PC1	819		846	753	831	879
PC3	812		848	746	819	881
PC5.2/2	876		933	826	891	969
PC12	858	844	885	784	–	919
Rftn31-2	965		939	828	953	975
Rftn31-3	863	846	890	787	827	925
Rftn43-1	904		938	844	921	974
Rftn43-7	870	892	918	819	892	953
Rftn43-9	864	869	903	800	865	938
Rftn55-1	884		926	830	900	961
Rftn55-2	869		901	809	903	935
Rftn57-2	816	821	857	768	824	890
Rftn57-3	872		904	808	870	939
JJG105	883		908	801	869	943
Rftn57-1	904		941	838	914	976
Rftn31-1	850		884	784	–	918
Rftn43-10	850		957	917	867	992
Rftn55-4	793		828	779	757	858
CMA1	833		868	839	766	898
CMA2	790		827	763	782	858
CMA14	832	812	861	800	791	893
CMA15	783		815	733	808	846

estimations and may add to the discrepancies between calibrations (Proyer et al. 2004). These discrepancies unfortunately cause significant uncertainty in depth of origin of the chemically distinct kyanite-bearing eclogites, and their location in relation to other eclogites.

Six orthopyroxene-bearing samples were used to evaluate the significance of T calculated by different mineral exchange reactions. These methods were compared at specified pressures of 20, 30 and 40 kbar, in order to eliminate complications introduced by barometer calibrations. The mean temperatures for all methods at the respective pressures are 814 ± 66, 850 ± 66 and 886 ± 69 (1σ)°C. The temperature range shown by each geothermometer is very different. For the thermometers based principally on Ca/Mg in clinopyroxene, T_{BKN} shows a range of ~270°C for the six samples, with T_{Ta} and T_{We} having somewhat smaller ranges of 170 and 130°C, respectively. The three diopside solvus thermometers (T_{We}, T_{BKN}, T_{Ta}) show generally poor agreement with one another, with differences up to 120°C for individual samples. This may reflect in part the differences in the ways that these formulations account for non-quadrilateral components, the discrepancies being accentuated above those normally observed for peridotites because the pyroxenes contain high jadeite components. The garnet-clinopyroxene Fe–Mg exchange thermometers (T_{EG}, T_{Kr}, T_{Be}) also show large ranges, from ~130 to ~150°C. In contrast, the orthopyroxene-based thermometers $T_{\mathrm{Ca\text{-}in\text{-}opx}}$ and T_{Ha} show much smaller total temperature ranges of 35 and 80°C, respectively. The mean temperatures from these latter two methods also coincide closely, e.g., 868 ± 14 and 872 ± 26°C at 30 kbar. There is a reasonable correlation of T_{EG} with T_{Ha} for all but one sample. These results indicate that although all methods yield broadly consistent temperatures, there is some uncertainty surrounding application of the thermometers involving Ca–Mg exchange in clinopyroxene to the Rietfontein opx-bearing eclogites.

Comparative geobarometry

Equilibration pressures for the orthopyroxene-bearing eclogites may be estimated using the Al-in-opx barometer. To assess the differences between barometer calibrations, independent of the choice of thermometer, calculated pressures were compared for an assumed temperature of 850°C (the mean temperature of all methods at 30 kbars). The Taylor (1998) (P_{Ta}) calibration yields the lowest pressure estimations; between 27.7 and 30.9 kbar, whereas estimations obtained using P_{BK} (Brey and Köhler 1990) give a range of 33.8–36.5 kbar. The average difference of ~6 kbar between the two methods probably reflects differences in the formulation of activity—composition relations and minor element corrections for these eclogites.

Table 10 Pressure-temperature estimates for orthopyroxene-bearing eclogites using various thermobarometer combinations

	PC5. 2/1	Rftn 56-1	CMA3	CMA11	CMA12	CMA13
P-BK	41.4	47.1	37.0	36.8	38.4	26.7
T-BKN	941	1050	892	876	883	739
P-BK	40.0	38.0	39.8	37.1	40.0	35.4
T-Ca in opx	918	906	928	882	909	873
P-BK	45.6	40.0	37.9	40.8	41.7	34.4
T-Ha84	1007	939	903	939	936	858
P-BK	42.8	38.5	32.3	40.4	47.8	31.9
T-EG79	962	914	831	933	1033	820
P-BK	34.0	30.0	24.0	31.9	39.8	24.9
T-Kr88	820	771	716	796	906	709
P-Ta98	25.6	31.5	33.9	23.5	21.3	23.6
T-Ta98	794	919	902	749	729	728
P-Ta98	30.3	28.7	34.0	29.1	28.7	30.6
T-Ca in opx	877	867	903	849	862	853
P-Ta98	33.2	29.5	29.3	32.3	35.8	28.1
T-EG79	928	883	821	905	988	808
P-Ta98	33.6	29.1	32.1	31.1	28.7	29.4
T-Ha84	935	876	871	884	862	830
P-Ta98	25.1	21.6	23.0	24.6	28.6	22.0
T-Kr88	785	739	713	768	860	699

BK, BKN and Ca in opx Brey and Kohler (1990), *Ha84* Harley (1984), *EG79* Ellis and Green (1979), *Kr88* Krogh (1988), *Ta98* Taylor (1998)

The experimental calibration of P_{Ta} in pyroxenitic bulk compositions more similar to eclogite than the peridotitic compositions of the P_{BK} calibration suggests that the former may be more accurate here.

Combined thermobarometry

Only the six orthopyroxene bearing samples are amenable to P–T estimates using thermobarometer combinations. Combinations of T_{BKN}, T_{Ta}, $T_{\mathrm{Ca\ in\ opx}}$, T_{EG}, T_{Kr} and T_{Ha} with P_{BK} and P_{Ta} were calculated (Table 10). These combinations result in a substantial spread of estimated P–T conditions, primarily as a result of divergent pyroxene solvus temperatures, and the systematic offset between barometer calibrations discussed above. The most extreme calculated P–T conditions are 699°C at 22 kbar (T_{Kr}–P_{Ta}) for CMA13 and 1,033°C, 47.8 kbar (T_{EG}–P_{BK}) for CMA12. Sample CMA13 records the lowest P–T conditions by most thermobarometer combinations. The mean for all samples and methods (i.e., 60 P–T determinations) is 863 ± 62°C, 32.9 ± 6.6 kbar. A preferred set of combinations that excludes the diopside solvus methods and T_{Kr} gives a mean of 878 ± 43°C at 30.8 ± 2.2 kbar.

Discussion

Petrographic comparisons with other eclogite suites

Petrographically, very few differences seem to exist between on-craton and off-craton eclogites. Textures are often very similar, and the same accessory minerals are found in eclogites from both tectonic settings. The Rietfontein eclogites are no exception. Granoblastic grain boundaries and triple junctions are common in lower crustal eclogites from Australia (Griffin and O'Reilly 1986) and South African on-craton localities such as Bellsbank (Taylor and Neal 1989). Spongy reaction rims around clinopyroxene grains are regularly reported from off-craton (Robey 1981; Pearson et al. 1995b) and on-craton (Taylor and Neal 1989; Beard et al. 1996; Snyder et al. 1997) eclogites and are commonly attributed to metasomatism, as are the frequently observed rims of secondary mica and amphibole around garnet grains (Taylor and Neal 1989). Some textural differences can be observed between the Rietfontein eclogites and other southern African off-craton localities. Kyanite in the Rietfontein kyanite eclogites always forms an interlocking textural arrangement with the garnet and clinopyroxene. Robey (1981) describes kyanite from the Cape Province eclogites as inclusions in garnet and clinopyroxene, acicular intergrowths with quartz, and as needle-like laths defining a foliation. Orthopyroxene from the Rietfontein eclogites is often altered, and is clearly different to the relict orthopyroxene and ''wormy'' trails of orthopyroxene found within clinopyroxene from the off-craton Cape Province suite eclogites (Robey 1981).

The Rietfontein eclogites show textures indicative of equilibrated rocks. Triple junctions are identifiable in many of the samples, together with straight grain boundaries. These triple junctions can be observed in all three groups, viz. bimineralic, orthopyroxene-bearing and kyanite eclogites. Triple junctions are representative of a metamorphic recrystallisation texture, and the granoblastic polygonal textures represent a close approach to textural equilibrium. Replacement textures are not exhibited by the Rietfontein eclogites and the described textures, together with homogeneous mineral grains, suggest that the xenolith suite is well equilibrated. These well-equilibrated textures and homogeneous chemical compositions contrast with the zoned mineral compositions and abundant evidence for mineralogical reactions in the lower crustal eclogite-granulite xenoliths from kimberlites that straddle the southwest margin of the Kaapvaal Craton (Robey 1981; Pearson et al. 1995b).

The kyanite eclogites are the freshest group of eclogites found at Rietfontein, a situation that contrasts with most cratonic eclogite suites (Gurney et al. 1971). In contrast, the bimineralic and orthopyroxene eclogites show varied degrees of alteration, and often contain secondary minerals such as phlogopite and amphibole. Spongy clinopyroxene rims which are present in some of the bimineralic and orthopyroxene eclogites are also absent in the kyanite eclogites. The lack of these minerals and textures in the kyanite eclogites suggests that they did not undergo the same metasomatic event to which the bimineralic and orthopyroxene eclogites were subjected. Furthermore, the common decomposition of jadeite-rich clinopyroxene of cratonic kyanite eclogites to a fine grained mixture prone to rapid alteration or melting (Berg 1968; Switzer and Melson 1969; Smyth 1980) is not observed in the Rietfontein eclogites. These factors may indicate that the latter derive from very shallow mantle levels, as predicted by the Berman et al. (1995) thermometer.

Chemical comparisons with other eclogite suites

Figure 2 shows fields for eclogitic garnets and clinopyroxenes from various on- and off-craton kimberlites in southern Africa. It is evident from Fig. 2a that garnets from the Rietfontein eclogites plot within the field defined by garnets from the on-craton Roberts Victor eclogites, whereas most lie outside the range of recorded compositions for off-craton eclogites. A similar pattern is evident for Cr, where garnets from the off-craton eclogite suite from Karoo kimberlites do not display the higher Cr contents seen in some of the Rietfontein and a number of on-craton eclogites.

Clinopyroxene compositions show that the Rietfontein eclogites exhibit a range in composition larger than that seen in off-craton eclogite suites (Fig. 2b), but within the range shown by on-craton suites (e.g. Orapa, Roberts Victor). Only the kyanite and high Na, Al eclogites have compositions that are recorded in off-craton eclogite suites. Major element mineral chemistry thus suggests that the Rietfontein eclogites are compositionally similar to on-craton eclogites. The high-Cr contents of some samples is a feature of cratonic eclogites and probably reflects a mantle origin, in that such samples may represent zones of interaction between eclogite bodies and their enclosing peridotite. Such material is absent in crustal eclogite suites perhaps because their wall rocks are not peridotitic. Similarly, the presence of orthopyroxene is not a feature of crustal eclogites, and may reflect hybridization with surrounding mantle. It is notable that the twofold compositional division of the Rietfontein eclogites is very similar to that seen for eclogites from the Koidu kimberlites, Sierra Leone, where Barth et al. (2001, 2002b) have recognised low- and high-MgO groups.

Nature of protolith

Eclogites are usually interpreted as either high-pressure metabasites, or as the direct crystallization of silicate melt at high pressure. Many eclogites appear to be samples of subducted oceanic crust emplaced tectonically into the lithospheric mantle (Helmstaedt and Doig 1975; Jagoutz et al. 1984; MacGregor and Manton 1986; Shervais et al. 1988; Taylor and Neal 1989; Neal et al. 1990; Jerde et al. 1993; Jacob et al. 1994; Viljoen et al. 1996; Snyder et al. 1997; Jacob and Foley 1999; Shirey et al. 2001), but substantial evidence for the high-pressure, magmatic origin has also been presented (MacGregor and Carter 1970; Hatton 1978; Smyth et al. 1989; Taylor et al. 1989, 2003; Neal et al. 1990; Caporuscio and Smyth 1990, Viljoen et al. 1996; Snyder et al. 1997; Barth et al. 2002b). Certain eclogites have been linked to partial melting and melt-mantle reaction processes associated with subduction, representing residues of tonalite melt extraction from basaltic crust (Ireland et al. 1994; Rollinson 1997; Barth et al. 2001, 2002a), or reaction products of tonalitic melts with peridotite (Taylor et al. 2003). The increasing recognition of ultra-high pressure metamorphism of continental crust must admit the possibility of eclogites with continental origins, and an origin by foundering or delamination of lower continental crust was suggested by Barth et al. (2002b) for a group of high-MgO eclogites from Koidu, West Africa. Metasomatism within the mantle after eclogite formation may also be significant (Ireland et al. 1994; Viljoen et al. 1996; Taylor et al. 1996; Snyder et al. 1997).

The Rietfontein eclogites show many textural and compositional characteristics that provide some insight into their geologic history. The minerals are all compositionally well-equilibrated, including the garnet exsolution lamellae in CMA1, indicating a substantial mantle residence period prior to kimberlite entrainment. Despite petrographic groupings of the eclogites as Group I and Group II eclogites (MacGregor and Carter 1970), Na_2O_{gt} and K_2O_{cpx} contents place all samples compositionally into Group II, as defined by McCandless and Gurney (1989). This suggests that the high degree of compositional and textural correspondence observed at Roberts Victor may not apply to off-craton mantle eclogites. With the possible exception of sample JJG2104, $\delta^{18}O$ values fall within the range for ultramafic upper mantle xenoliths of 5.5 ± 0.7‰ (Mattey et al. 1994).

Barth et al. (2001, 2002b) have recently reported on a detailed study of eclogites from Koidu in West Africa, and recognize two distinct groups with respect to calculated bulk rock compositions, one with low-MgO (containing kyanite) the other with high-MgO. The compositions of these two groups are remarkably similar to the kyanite eclogites (low-MgO) and bimineralic eclogites (high-MgO) from Rietfontein. The latter in particular are indistinguishable in terms major element compositions.

Figure 5 shows calculated bulk rock compositions of the Rietfontein eclogites, and it is clear that the bimineralic eclogites have compositions unlike mid-ocean ridge basalts, but fall comfortably within the field of oceanic gabbros and pyroxenite veins from ophiolite complexes. They tend to be slightly less MgO-rich than Archean picrites and komatiites, and are more Al_2O_3 and CaO-rich and less TiO_2-rich than either Archean picrites or basalts, although the low TiO_2 may be a reflection of the absence of rutile or ilmenite in the bulk rock calculation. They are clearly lower in SiO_2 and richer in CaO and Al_2O_3 than boninites. The reconstructed bulk rock compositions of the Rietfontein bimineralic eclogites are indistinguishable in terms of their major elements from the high-MgO group of eclogites recognized by Barth et al. (2002b) from Koidu, West Africa. The raised MgO and CaO, and to lesser extent Al_2O_3 contents of the Rietfontein bimineralic eclogites suggest a cumulate origin, and following arguments presented by Barth et al. (2002b) regarding flat HREE patterns (Fig. 6), would appear to be low pressure pyroxene-olivine-(±) plagioclase cumulates, rather than garnet-pyroxene cumulates. The inferred metagabbroic-pyroxenitic protolith to the Rietfontein bimineralic eclogites could represent either the basal section of subducted oceanic crust, or foundered mafic lower continental crust. The flat to slightly raised LREE patterns of the Rietfontein bimineralic eclogites (Fig. 6) are atypical of oceanic gabbros, and the relative enrichment in LREE and other incompatible elements (Fig. 7) argue also against having experienced partial melting relating to Archean subduction and TTG generation, as has been proposed for some eclogite suites (e.g. Ireland et al. 1994; Jacob et al. 1994; Helmstaedt and Doig 1975; MacGregor and Manton 1986), unless subsequent metasomatism has re-enriched the incompatible trace elements.

It is clear that the kyanite eclogites are significantly poorer in SiO_2 and richer in Al_2O_3 than typical MORB, boninites or most oceanic gabbros (Fig. 5); they are also clearly distinct from Archean mafic and picritic rocks. The strong positive Eu and Sr anomalies in reconstructed bulk rock compositions (Figs. 6, 7) make the kyanite eclogites strong candidates for having had a low pressure, plagioclase-rich, protolith. The strong LREE and incompatible element depletion points towards an oceanic crustal protolith, which would need to be rich in calcic plagioclase and olivine (the only two primary low-SiO_2 minerals in oceanic crust), to cause an overall low SiO_2 content in the bulk rock (perhaps a body of troctolite—a not uncommon rock-type in the oceanic crustal section). Alternatively, the very strong depletion in incompatible elements might point to a protolith that is the plagioclase-olivine rich residue of a prior partial melting event. A number of authors have argued for eclogites to represent residual oceanic crust that lost melt to form TTG suites during the Archean (e.g. Ireland et al. 1994; Jacob et al. 1994). Assuming a residual Ti-bearing phase, such residues would be expected to be relatively enriched in Nb, Ta and Ti (e.g. Barth et al. 2001) which is not evident in Rietfontein kyanite eclogites (Fig. 7). However, inclusion of <0.2% rutile or ilmenite in the calculated bulk rock compositions would cause the kyanite eclogites to have very strong positive Nb and Ta anomalies, making it a significant possibility that the Rietfontein kyanite eclogites represent remnants of old oceanic crust that was partially dehydrated and melted during subduction during the Archean.

P–T Conditions of eclogite origin

The range of *P–T* conditions inferred from the preferred thermobarometer combinations for the orthopyroxene-bearing eclogites places the origin of these xenoliths within the mantle, at a depth range of 85–115 km. Although crustal thickness in this area is not well known, a typical thickness for crust in the Proterozoic terranes west of the Kaapvaal Craton is ~40 km (Nguuri et al. 2001). A mantle origin is consistent with a lack of plagioclase in any of the samples. Homogeneous mineral compositions in most samples suggest that the estimated conditions apply to the time of sampling by the kimberlite, and were not frozen in during cooling to substantially lower temperatures. By way of contrast, Boyd et al. (1999) showed that spinel peridotites from the shallowest portion of the Kaapvaal craton upper mantle (35–70 km) do not preserve homogeneous orthopyroxene compositions, and furthermore commonly exhibit exsolution textures.

Garnet-clinopyroxene temperatures [T_{EG}] of the orthopyroxene-bearing eclogites are on average at the lower end of the Rietfontein eclogite range and the kyanite-bearing samples are clustered towards the high end. The range of calculated temperatures of all the eclogites at an assumed pressure of 30 kbar is 815–1,012°C. These temperatures correspond to a depth range of 95–125 km, assuming an average Kalahari geotherm (see below). The range begins at slightly greater depths than inferred for the opx-bearing eclogites because the T_{EG} estimates are generally higher than the mean of T_{Ha}, $T_{Ca\text{-}in\text{-}opx}$, and T_{EG} used to estimate opx-eclogite *P–T* conditions. Although the kyanite-bearing samples are apparently clustered at the high end of the range (105–125 km), the vast composition-dependent differences between the three calibrations of the gt-cpx thermometer, and the potential for variations in Fe^{3+} between the different chemical groups, suggest that little certainty can be attached to this rough stratigraphic arrangement of rock types. It is possible that all the eclogites have a similar depth of origin, although this cannot be confirmed until the origins of the discrepancies between thermobarometric methods are better understood.

The range of temperatures calculated for the Rietfontein eclogites is substantially lower than that of many eclogite suites derived from the mantle below the Kaapvaal craton. Figure 8 compares the equilibration temperatures of the Rietfontein eclogites (*a*) with temperatures from the Cape Province off-craton eclogites (*b*), and on-craton localities Bellsbank (*c*), Udachnaya (*d*), Roberts Victor (*e*& *f*) and Kaalvallei (*g*& *h*). For all localities, temperatures were calculated using T_{EG} at an assumed pressure of 30 kbar. The range of temperatures, and temperature distribution of the Rietfontein eclogites is very similar to that of the Cape Province off-craton eclogites of Robey (1981). Both exhibit temperature distribution maxima between 900 and 950°C, but the Cape Province eclogites extend to lower equilibration temperatures (755°C) than the Rietfontein eclogites, and furthermore are known to derive from substantially lower pressures (Robey 1981; Pearson et al. 1995b; Schmitz and Bowring 2003). The Bellsbank eclogites (*c*) have a restricted temperature range (although this may be due to a restricted number of temperature determinations), with most temperatures ranging from 1,000 to 1,100°C. On-craton Russian eclogites, represented by Udachnaya (*d*), extend to higher temperatures than the South African off-craton eclogites and most temperatures fall between 950 and 1,000°C. However, the temperature range is very similar to that of the Obnazhennaya suite, which derives from the NE margin of the Siberian platform (Taylor et al. 2003). Roberts Victor eclogites (*e*& *f*) show the largest temperature distribution, from 770 to 1,363°C, at 30 kbar, although the majority of temperatures range from 1,050 to 1,100°C. Eclogites from Kaalvallei also exhibit a wide temperature range, with a maximum temperature distribution from 1,050 to 1,100°C.

Figure 8 illustrates the greater range of equilibration temperatures and higher average temperatures of on-craton eclogites, when compared to Rietfontein. Griffin and O'Reilly (1986) suggest that xenoliths from east Australia that have equilibration temperatures less than 850°C may be regarded as crustal xenoliths. A number of Rietfontein eclogites have calculated equilibration temperatures less than this, but if these were crustal xenoliths, there should be petrographic and chemical differences between these eclogites and those of higher temperature origin, which are likely to be mantle-derived. However, such systematic differences within the suite are not apparent, and it is thus likely that the Rietfontein eclogites are all mantle-derived, with the similarity in temperature range to lower crustal eclogites largely coincidental. The inferred shallow depths of origin of the Rietfontein eclogites implies that any carbon present in these rocks would occur as graphite, consistent with the apparent lack of diamond at Rietfontein.

Thermal structure of the lithosphere beneath Rietfontein

Pressures and temperatures obtained from the orthopyroxene-bearing eclogites may be used to place constraints on the thermal structure of the lithosphere in the Rietfontein area at the time of kimberlite eruption (~70 Ma). Figure 9 illustrates these data calculated according to six different thermobarometer combinations, and compares the results to model continental geotherms of Pollack and Chapman (1977), and to the Kalahari geotherm of Rudnick and Nyblade (1999). The Kalahari geotherm is a best fit to the P_{BK}–T_{BKN} data array for cratonic xenoliths from southern Africa. In addition, the temperatures and pressures of peridotite xenoliths from the Gibeon kimberlites in Namibia, which are geographically the closest mantle samples available for which *P*–*T* data exist (Boyd et al. 2004), and also constitute the most extensively studied suite of samples derived from mantle beneath Proterozoic crust in southern Africa, have been plotted.

The *P*–*T* arrays in Fig. 9a–f display substantial differences and provide useful information on the probable accuracy of thermobarometer pairs. All three arrays based on P_{BK} lie below the Kalahari geotherm, whereas the P_{Ta} arrays lie on or slightly above it. Furthermore, the P_{BK}-based arrays lie below most *P*–*T* data calculated for southern African xenoliths according to the same thermobarometer combinations, whereas P_{Ta} arrays do not. This suggests either that the Rietfontein xenoliths are anomalously cool compared with most others in southern Africa (but not all—Bell 2002; Michaut et al. 2007) or, more likely, that the application of P_{BK} to these xenoliths is problematic because of its inappropriate formulation for these fertile eclogite-websterite compositions (Taylor 1998). Although the absolute accuracy of P_{Ta}-based *P*–*T* data remains unconfirmed, these data appear to provide a better basis for comparison to other xenoliths.

The three P_{Ta}-based sets of *P*–*T* data (Fig. 9d–f) all suggest that the Rietfontein eclogites equilibrated close to the average Kalahari geotherm defined by cratonic peridotite xenoliths. Comparison with theoretical models assuming average crustal compositions suggests that this array corresponds to a surface heat flow in the region of 41–42 mW m^{-2} (Rudnick and Nyblade 1999; Rudnick et al. 1998). The Kalahari *P*–*T* array also forms the low-temperature bound to peridotites from the Gibeon kimberlites, which extend from the cratonic array to higher, perturbed temperatures (Mitchell 1984; Bell et al. 2003). There is, however, no evidence of thermal perturbation in the Rietfontein eclogites. The Rietfontein eclogites there-

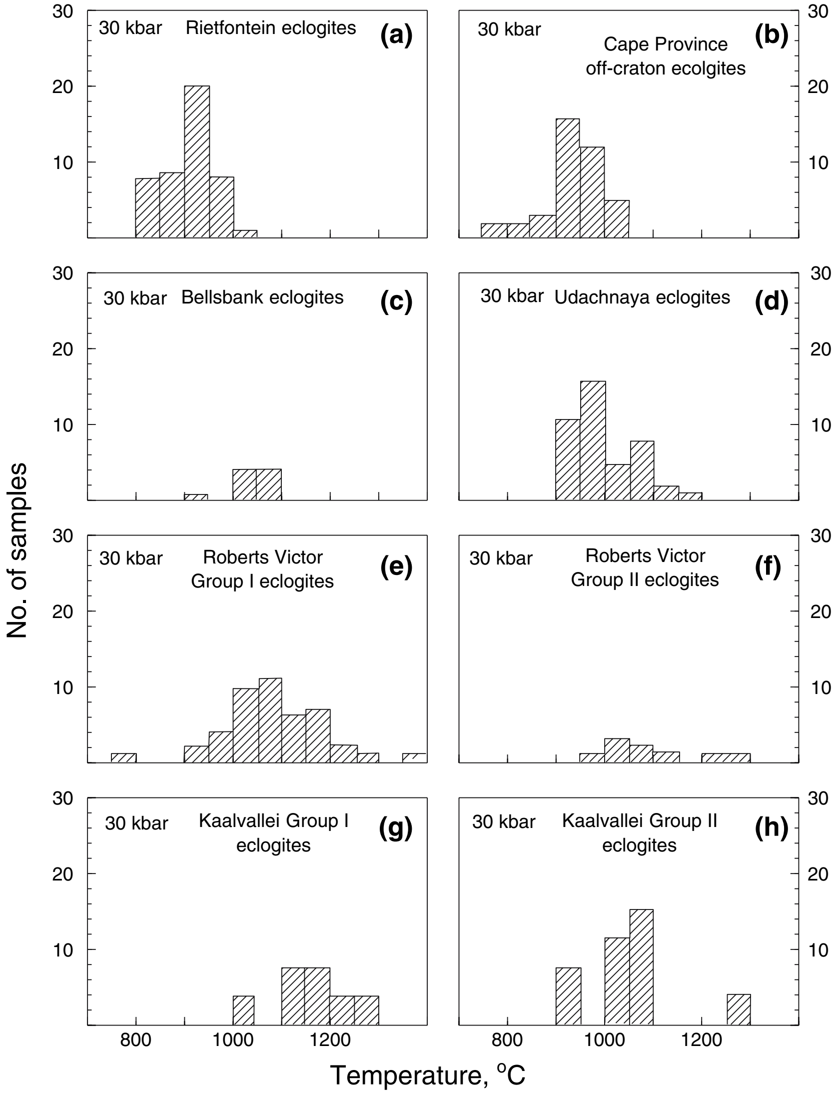

Fig. 8 Comparative histograms showing calculated equilibrium temperatures (at 30 kbar) using Ellis and Green (1979) for Rietfontein eclogites and for a number of other on- and off-craton eclogite localities. Sources of data: Robey (1981); MacGregor and Manton (1986); Viljoen (1994, 1995); Jacob et al. (1994); Snyder et al. (1997)

fore provide further evidence for the existence of ''cratonic'' thermal conditions in ''off-craton'' lithosphere in southern Africa, following cooling after the Namaqua-Natal thermotectonic event (Bell et al. 2003; Schmitz and Bowring 2003).

These thermal conditions in the Mesozoic differ from those suggested by the average present-day heat flow for Proterozoic terrains in southern Africa, which are 61 ± 10 mW m^{-2} in the Namaqua-Natal belt, and 63 ± 6 mW m^{-2} in the Ghanzi-Chobe belt (Jones 1987). Interpolation of measurements surrounding the Rietfontein area (Jones 2001) suggests similar values, although there is much evidence for local variability, typically caused by variations in crustal heat production (Jaupart and Mareschal 1999). The higher average surface heatflow is partly due to thicker crust in Proterozoic domains, but is also likely to contain an excess mantle-derived component (Jones 2001). Indications of a time-dependent transition to such higher temperature conditions in the mantle are given by the *P*–*T* arrays in Namibia, East Griqualand and the younger kimberlites in Eastern Namaqualand (Bell et al. 2003). For example, peridotites from Louwrensia indicate an average ''geotherm'' close to 44 mW m^{-2} (Pearson et al. 1994) and Anis Kubub peridotites yield ''geotherms'' of 44–50 mW m^{-2} (Franz et al. 1996), despite several samples recording lower temperatures. These highly scattered *P*–*T* arrays are considered transient phenomena resulting from the advection of magmatic heat to various levels in the lithosphere.

Summary and conclusions

The Rietfontein eclogites exhibit relatively simple mineralogies and textures. On a textural basis Group II eclogites account for 61% of the suite, Group I eclogites 13%, with

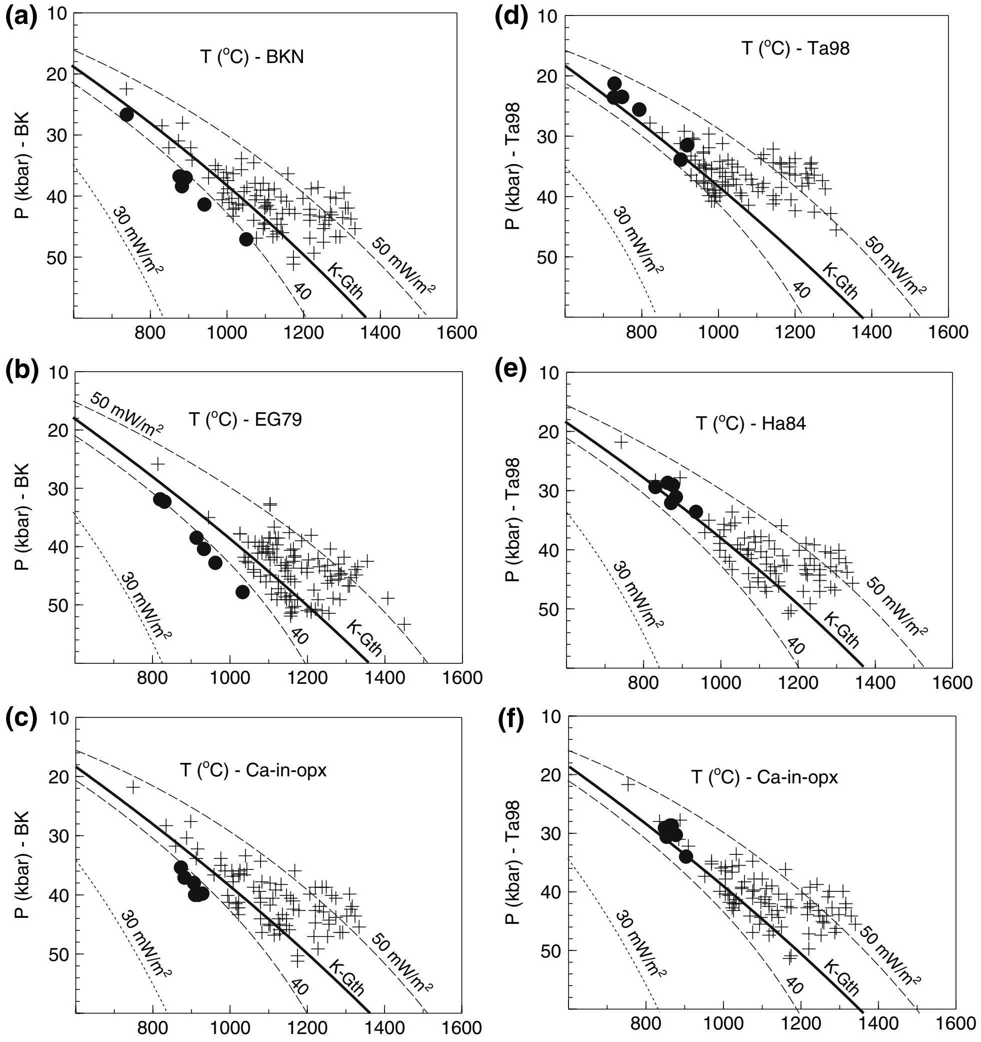

Fig. 9 Calculated *P–T* data for Rietfontein orthopyroxene eclogites and Gibeon peridotites (Pearson et al. 1994; Franz et al. 1996) using six different thermobarometer combinations. Superimposed geotherms from Rudnick and Nyblade (1999; *K-Gth* Kalahari geotherm) and Pollack and Chapman (1977; 30, 40 and 50 mW m^{-2}); the latter calculated for a number of different heat flow values

26% of the suite indeterminate. Textures and homogeneous chemical compositions of minerals indicate equilibrated rocks. The presence of garnet exsolution lamellae in pyroxene indicates a higher temperature history for some bimineralic eclogite samples, consistent with proposals (e.g. Barth et al. 2002b) that some high-MgO eclogites could represent high pressure cumulates. At the low temperatures indicated by mineral thermometers, the chemical equilibration of these lamellae indicates substantial mantle residence times. The kyanite eclogites are unusually fresh and could derive from a shallower mantle region.

On a chemical basis, the Rietfontein eclogites can be classified as Group A and Group B eclogites after Taylor and Neal (1989). Group B eclogites include the kyanite and orthopyroxene-bearing eclogites, with the bimineralic eclogites forming the bulk of the Rietfontein Group A eclogites. Many of the Rietfontein Group A eclogites contain garnets and clinopyroxenes with relatively high Cr_2O_3 contents (>0.4–0.5 wt%) suggesting a mantle crystallization environment, or dispersal of small eclogite bodies in the mantle.

Bulk compositions of the Rietfontein eclogites suggest a two-fold subdivision into MgO-rich and MgO-poor eclogites, similar to that observed for Koidu eclogites (Barth et al. 2001, 2002b). Kyanite-bearing eclogites and kyanite-free eclogites with similar mineral chemistry comprise the low MgO-group, also characterized by low incompatible trace element concentrations, strong LREE depletion, positive Eu and Sr anomalies, and high Al_2O_3 and low SiO_2 relative to mid-ocean ridge basalt. All these features are consistent with a plagioclase-rich precursor, which on the basis of SiO_2 content is most likely to have been troctolitic. In the absence of further chemical indicators, this could represent the feldspathic cumulate portion of the oceanic crust, perhaps the remnant of melt extraction during Archean crust formation. By way of contrast, the high-MgO, bimineralic eclogites have less depleted LREE and incompatible element concentrations, and appear to have had a gabbroic or pyroxenitic protolith that could have derived either from the basal section of subducting oceanic crust, or from foundered/delaminated mafic lower continental crust. Group II eclogites from elsewhere in southern Africa record radiogenic Sr isotope ratios that suggest either continental lithospheric (crust or mantle) input, or metasomatism (Neal et al. 1990; Viljoen et al. 1996).

On the balance of evidence, the observations presented here can be interpreted in terms of a subducted oceanic lithosphere component, including feldspathic and olivine-gabbro cumulates, and mantle with included pyroxenites, or in terms of lithologically complex continental lithosphere containing pyroxenitic cumulates from mafic magmas, and tectonically juxtaposed mafic material from overlying lower crust. A local example of complex imbrication of crust and mantle, preserved over >2 Ga is evident in the disrupted Moho imaged seismically in the Limpopo Belt (Nguuri et al. 2001). The resolution between these two scenarios and their integration into a model for tectonic evolution of the lithosphere of the Rehoboth subprovince should be improved by radiogenic isotope studies of these eclogites and their associated mantle peridotites, and by a study of associated peridotitic xenoliths and xenocrysts.

Acknowledgments Financial support for this work was provided by the National Research Foundation of South Africa, the University of Cape Town and De Beers. DRB acknowledges additional support from National Science Foundation Grants EAR-0310330 and EAR-0538320. Constructive reviews by Graham Pearson and Clive Neal improved the final version of this manuscript and are greatly appreciated.

References

Barth MG, Rudnick RL, Horn I, McDonough WF, Spicuzza MJ, Valley JW (2001) Geochemistry of xenolithic eclogites from West Africa; Part I, A link between low MgO eclogites and Archean crust formation. Geochim Cosmochim Acta 65:1499–1527

Barth MG, Rudnick RL, Carlson RW, Horn I, McDonough WF (2002a) Re-Os and U-Pb geochronological constraints on the eclogite-tonalite connection in the Archean Man Shield, West Africa. Precambrian Res 118:267–283

Barth MG, Rudnick RL, Horn I, McDonough WF, Spicuzza MJ, Valley JW, Haggerty SE (2002b) Geochemistry of xenolithic eclogites from West Africa; Part 2, Origins of the high-MgO eclogites. Geochim Cosmochim Acta 66:4325–4345

Beard BL, Fraracci KN, Taylor LA, Snyder GA, Clayton RA, Mayeda TK, Sobolev NV (1996) Petrography and geochemistry of eclogites from the Mir kimberlite, Yakutia, Russia. Contrib Mineral Petrol 125:293–310

Bell DR (2002) Mesozoic thermal evolution of the Kaapvaal Craton mantle root. Eos Trans AGU, 83(47), Fall Meet Suppl, Abstract T61A–1243

Bell DR, Rossman GR (1992) The distribution of hydroxyl in garnets from the subcontinental mantle of southern Africa. Contrib Mineral Petrol 111:161–178

Bell DR, Schmitz MD, Janney PE (2003) Mesozoic thermal evolution of the southern African mantle lithosphere. Lithos 71:273–287

Berg GW (1968) Secondary alteration in eclogites from kimberlite pipes. Am Mineral 53:1336–1346

Berman RG, Aranovich LY, Pattison DRM (1995) Reassessment of the garnet-clinopyroxene Fe-Mg exchange thermometer: II Thermodynamic analysis. Contrib Mineral Petrol 119:30–42

Bloomer SH (1989) Geochemical characteristics of boninite- and tholeiite-series rocks of the Mariana forearc and the role of an incompatible element-enriched fluid in arc petrogenesis. In: Morris EM, Pasteris JD (eds) Mantle metasomatism and alkaline magmatism. Geol Soc Amer Spec Paper 215:151–164

Boyd FR, Pearson DG, Mertzman SA (1999) Spinel facies peridotites from the Kaapvaal root. In: Gurney JJ et al. (eds) The J. B. Dawson Volume. Proceedings of the seventh Internat Kimberlite Conf Vol. 1 Red Roof Design, Cape Town, pp 40–48

Boyd FR, Pearson DG, Hoal KO, Hoal BG, Nixon PH, Kingston MJ, Mertzman SA (2004) Garnet lherzolites from Louwrensia, Namibia: bulk composition and *P*/*T* relations. Lithos 77:573–592

Brey GP, Köhler T (1990) Geothermobarometry in Four-phase Lherzolites. II. New thermobarometers, and practical assessment of existing thermobarometers. J Petrol 31:1353–1378

Brown AV, Jenner GA (1989) Geological setting, petrology and chemistry of Cambrian boninite and low-Ti tholeiite lavas in western Tasmania. In: Crawford AJ (Ed) Boninites. Unwin Hyman, pp 232–263

Caporuscio FA, Smyth JR (1990) Trace element crystal chemistry of mantle eclogites. Contrib Mineral Petrol 105:550–561

Carswell DA (1990) Eclogites and the eclogite facies: definitions and classifications. In: Carswell DA (ed) Eclogite facies rocks. Blackie, pp 1–13

Coish RA (1989) Boninitic lavas in Appalachian ophiolites: a review. In: Crawford AJ (ed) Boninites. Unwin Hyman, pp 264–287

Davies GR, Spriggs AJ, Nixon PH (2001) A non-cognate origin for the Gibeon kimberlite megacryst suite, Namibia: implications for the origin of Namibian kimberlites. J Petrol 42:159–172

Davis GL, Krogh TE, Erlank AJ (1976) The ages of zircons from kimberlites from South Africa Carnegie Inst Washington Yearb 75:821–824

Dawson JB (1989) Geographic and time distribution of kimberlites and lamproites: relationships to tectonic processes. In: Ross J, Jaques AL, Ferguson J, Green DH, O'Reilly SY, Danchin RV, Janse AJA (eds) Kimberlites and related rocks: their composition, occurrence, origin and emplacement. Geol Soc Australia Spec Publ 14:323–342

Dawson JB, Smith JV (1987) Reduced sapphirine granulite xenoliths from the Lace kimberlite, South Africa; implications for the deep structure of the Kaapvaal Craton. Contrib Mineral Petrol 95:376–383

Dawson JB, Carswell DA (1990) High temperature and ultra-high pressure eclogites In: Carswell DA (Ed) Eclogite facies rocks. Blackie, pp 315–349

Droop GT (1987) A general equation for estimating Fe^{3+} concentrations in ferromagnesian silicates and oxides from microprobe analyses, using stoichiometric criteria. Min Mag 51:431–435

Ellis DJ, Green DH (1979) An experimental study of the effect of Ca upon garnet-clinopyroxene Fe-Mg exchange equilibria. Contrib Mineral Petrol 71:13–22

Franz L, Brey G, Okrusch M (1996) Steady state geotherm, thermal disturbances, and tectonic development of the lower lithosphere underneath the Gibeon Kimberlite Province, Namibia. Contrib Mineral Petrol 126:181–198

Griffin WL, O'Reilly SY (1986) The lower crust in eastern Australia: Xenolith evidence. In: Dawson JB, Carswell DA, Hall J, Wedepohl KH (eds) The nature of the lower continental crust. Geol Soc Lond Spec Publ 24:363–374

Griffin WL, Carswell DA, Nixon PH (1979) Lower-crustal granulites and eclogites from Lesotho, Southern Africa. In: Boyd FR, Meyer HOA (eds) The mantle sample; inclusions in kimberlites and other volcanics. Proceedings of the second international Kimberlite conference 2:59–86

Gurney JJ (1984) A correlation between garnets and diamonds. In Glover JE, Harris PG (eds) Kimberlite occurrence and origin: a basis for conceptual models in exploration. Geology Department and University Extension, Univ Western Australia Publ 8:143–166

Gurney JJ, Harte B (1980) Chemical variations in upper mantle nodules from southern African kimberlites. Philos Trans R Soc Lond A297:273–293

Gurney JJ, Mathias M, Siebert C, Moseley G (1971) Kyanite eclogites from the Rietfontein kimberlite pipe, Mier Coloured reserve, Gordonia, Cape Province, South Africa. Contrib Mineral Petrol 30:46–52

Haggerty SE (1991) Oxide mineralogy of the upper mantle. In: Lindsley DH (Ed) Oxide minerals: petrologic and magnetic significance. Rev Mineral 25:355–416

Harley SL (1984) An experimental study of the partitioning of Fe and Mg between garnet and orthopyroxene. Contrib Mineral Petrol 86:359–373

Harris C, Smith HS, le Roex AP (2000) Oxygen isotope composition of phenocrysts from Tristan da Cunha and Gough Island lavas: variation with fractional crystallization and evidence for assimilation. Contrib Mineral Petrol 138:164–175

Harte B, Gurney JJ (1975) Evolution of clinopyroxene and garnet in an eclogite nodule from the Roberts Victor kimberlite pipe, South Africa. In: Ahrens LH, Dawson JB, Duncan AR, Erlank AJ (eds) Phys Chem Earth 9:367–387

Hartnady C, Joubert P, Stowe C (1985) Proterozoic crustal evolution in Southwestern Africa. Episodes 8:236–244

Hatton CJ (1978) The geochemistry and origin of xenoliths from the Roberts Victor Mine. PhD thesis, University of Cape Town, South Africa

Helmstaedt H, Doig R (1975) Eclogite nodules from kimberlite pipes of the Colorado Plateau—samples of subducted Franciscan-type oceanic lithosphere. In: Ahrens LH, Dawson JB, Duncan AR, Erlank AJ (eds) Phys Chem Earth 9:95–111

Ireland TR, Rudnick RL, Spetsius Z (1994) Trace elements in diamond inclusions from eclogites reveal link to Archean granites. Earth Planet Sci Lett 128:199–213

Jacob DE (2004) Nature and origin of eclogite xenoliths from kimberlites. Lithos 77:295–316

Jacob D, Foley SF (1999) Evidence for Archean ocean crust with low field strength element signature from diamondiferous eclogite xenoliths. Lithos 48:317–336

Jacob D, Jagoutz E, Lowry D, Mattey D and Kudrjavtseva G (1994) Diamondiferous eclogites from Siberia: remnants of Archean oceanic crust. Geochim Cosmoschim Acta 58:5191–5207

Jagoutz E, Dawson JB, Hoernes S, Spettel B, Wänke H (1984) Anorthositic oceanic crust in the Archaean Earth. In: Fifteenth Lunar Planet Sci Conf, Houston, pp 395–396

Janney PE, le Roex AP, Carlson RW, Viljoen KS (2002) A chemical and multi-isotope study of the Western Cape olivine melilitite province, South Africa: implications for the sources of kimberlites and the origin of the HIMU signature in Africa. J Petrol 43:2339–2370

Jaupart C, Mareschal JC (1999) The thermal structure and thickness of continental roots. Lithos 48:93–114

Jerde EA, Taylor LA, Crozaz G, Sobolev NV, Sobolev VN, (1993) Diamondiferous eclogites from Yakutia, Siberia: evidence for a diversity of protoliths. Contrib Mineral Petrol 114:189–202

Jones MQW (1987) Heat flow and heat production in the Namaqua Mobile Belt, South Africa. J Geophys Res 92:6273–6289

Jones MQW (2001) A review of heat flow in Southern Africa and the thermal structure of the Kaapvaal lithosphere. The Slave-Kaapvaal workshop, Extended Abstracts, pp 106–111

Kerrich R, Wyman D, Fan J, Bleeker W (1998) Boninite series: low Ti-tholeiite associations from the 2.7 Ga Abitibi greenstone belt. Earth Planet Sci Lett 164:303–316

Kramers JD (1979) Lead, uranium, strontium, potassium and rubidium in inclusion-bearing diamonds and mantle-derived xenoliths from southern Africa. Earth Planet Sci Lett 42:58–70

Krogh EJ (1988) The garnet-clinopyroxene Fe-Mg geothermometer—a reinterpretation of existing experimental data. Contrib Mineral Petrol 99:44–48

Kurszlaukis S, Franz L, Lorenz V (1998) On the volcanology of the Gibeon Kimberlite Field, Namibia. J Volc Geoth Res 84:257–272

le Roex AP, Dick HJB, Erlank AJ, Reid AM, Frey FA, Hart SR (1983) Geochemistry, mineralogy and petrogenesis of lavas erupted along the South-West Indian Ridge between the Bouvet triple junction and 11°E. J Petrol 24:267–318

le Roex AP, Dick HJ, Reid AM, Frey FA, Erlank AJ (1985) Petrology and geochemistry of basalts from the American-Antarctic Ridge, Southern Ocean: implications for the west-ward influence of the Bouvet mantle plume. Contrib Mineral Petrol 90:367–380

le Roux PJ, le Roex AP, Schilling JG (2002) Crystallisation beneath the southern Mid-Atlantic Ridge (40°–55°S), evidence for high pressure of initiation of crystallization. Contrib Mineral Petrol 142:582–602

MacGregor ID, Carter JL (1970) The chemistry of clinopyroxenes and garnets of eclogite and peridotite xenoliths from the Roberts Victor Mine, South Africa. Phys Earth Planet Int 3:391–397

MacGregor ID, Manton WI (1986) Roberts Victor eclogites: ancient oceanic crust. J Geophys Res 91:14063–14079

Mattey D, Lowry D, MacPherson C (1994) Oxygen isotope composition of mantle peridotite. Earth Planet Sci Lett 128:231–241

McCandless TE, Gurney JJ (1989) Sodium in garnet and potassium in clinopyroxene: criteria for classifying mantle eclogites. In: Ross J (Ed) Kimberlites and related rocks. Vol 2 Their mantle/crust setting, diamonds and diamond exploration. Geol Soc Australia Spec Publ 14 Blackwell, Carlton, pp 827–832

Michaut C, Jaupart C, Bell DR (2007) Transient geotherms in Archean continental lithosphere: new constraints on thickness and heat production of the subcontinental lithospheric mantle. J Geophys Res (in press)

Mitchell RH (1984) Garnet lherzolites from the Hanaus-I and Louwrensia kimberlites of Namibia. Contrib Mineral Petrol 86:178–188

Morimoto N (1988) Nomenclature of pyroxnenes. Am Mineral 73:1123–1133

Neal CR, Taylor LA, Davidson JP, Holden P, Halliday AN, Nixon PH, Paces JP, Clayton RN, Mayeda TK (1990) Eclogites with oceanic crustal and mantle signatures from the Bellsbank kimberlite, South Africa, part 2: Sr, Nd, and O isotope geochemistry. Earth Planet Sci Lett 99:362–379

Nguuri TK, Gore J, James DE, Webb SJ, Wright C, Zengeni TG, Gwavava O, Snoke JA (2001) Crustal structure beneath southern Africa and its implications for the formation and evolution of the Kaapvaal and Zimbabwe cratons. Geophys Res Lett 28:2501–2504

Pearson DG, Boyd FR, Hoal KEO, Hoal BG, Nixon PH, Rogers NW (1994) A Re-Os isotopic and petrological study of Namibian peridotites: contrasting petrogenesis and composition of on- and off-craton lithospheric mantle. Mineral Mag 58A:703–704

Pearson DG, Snyder G A, Shirey SB, Taylor LA, Carlson RW, Sobolev NV (1995a) Archaean Re-Os age for Siberian eclogites and constraints on Archaean tectonics. Nature 374:711–713

Pearson NJ, O'Reilly SY, Griffin WL (1995b) The crust-mantle boundary beneath cratons and craton margins: a transect across the south-west margin of the Kaapvaal craton. Lithos 36:257–287

Pollack HN, Chapman DS (1977) On the regional variation of heat flow, geotherms, and lithospheric thickness. Tectonophysics 38:279–296

Pouchou JL, Pichoir F (1991) Quantitative analysis of homogeneous or stratified microvolumes applying the model 'PAP'. In: Heinrich KFJ, Newbury DE (eds) Electron probe quantitation. Plenum, New York, pp 31–76

Proyer A, Dachs E, McCammon C (2004) Pitfalls in the geothermobarometry of eclogites: Fe^{3+} and changes in the mineral chemistry of omphacite at ultrahigh pressures. Contrib Mineral Petrol 147:305–318

Richardson SH, Shirey SB, Harris JW, Carlson RW (2001) Archean subduction recorded by Re-Os isotopes in eclogitic sulfide inclusions in Kimberley diamonds. Earth Planet Sci Lett 191:257–266

Rickwood PC, Gurney JJ, White-Cooper DR (1969) The nature and occurrences of eclogite xenoliths in the kimberlites of Southern Africa. In: The Upper Mantle Project, Geol Soc S Afr Spec Publ 2:371–394

Robey JV (1981) Kimberlites of the Central Cape Province, RSA. PhD thesis, University of Cape Town, South Africa

Rogers NW, Hawkesworth CJ (1982) Proterozoic age and cumulate origin for granulite xenoliths, Lesotho. Nature 299:409–413

Rollinson H (1997) Eclogite xenoliths in west African kimberlites as residues from Archean granitoid crust formation. Nature 389:173–176

Rudnick RL, Nyblade AA (1999) The thickness and heat production of Archean lithosphere: constraints from xenolith thermobarometry and surface heat flow. In: Fei Y, Bertka C, Mysen BO (eds) Mantle petrology: field observations and high-pressure experimentation: a tribute to Francis R (Joe) Boyd. Geochem Soc Spec Publ 6:3–12

Rudnick RL, McDonough WF, O'Connell RJ (1998) Thermal structure, thickness and composition of continental lithosphere. Chem Geol 145:395–411

Sautter V, Harte B (1988) Diffusion gradients in an eclogite xenolith from the Roberts Victor kimberlite pipe: (1) mechanism and evolution of garnet exsolution in Al_2O_3-rich clinopyroxene. J Petrol 29:1325–1358

Schmitz MD, Bowring SA (2003) Constraints on the thermal evolution of tcontinental lithosphere from U-Pb accessory mineral thermochronometry of lower crustal xenoliths, southern Africa. Contrib Mineral Petrol 144:592–618

Schmitz MD, Bowring SA (2004) Lower crustal granulite formation during Mesoproterozoic Namaqua-Natal collisional orogenesis, southern Africa. Trans Geol Soc S Afr 107:261–284

Schulze DJ (1989) Constraints on the abundance of eclogite in the upper mantle. J Geophys Res 94:4205–4212

Shee SR (1978) The mineral chemistry of xenoliths from the Orapa kimberlite pipe, Botswana. Unpubl MSc thesis, University of Cape Town

Shervais JW, Taylor LA, Lugmair GW, Clayton RN, Mayeda TK, Korotev RL (1988) Early Proterozoic oceanic crust and the evolution of subcontinental mantle: eclogites and related rocks from southern Africa. Geol Soc Amer Bull 100:411–423

Shirey SB, Carlson RW, Richardson SH, Menzies AH, Gurney JJ, Pearson DG, Harris JW, Wiechert U (2001) Archean emplacement of eclogitic components into the lithospheric mantle during formation of the Kaapvaal Craton. Geophys Res Lett 28:2509–2512

Smith D (1999) Temperatures and pressures of mineral equilibration in peridotite xenoliths: review, discussion, and implications. In: Fei Y, Bertka CM, Mysen BO (eds) Mantle petrology: field observations and high pressure experimentation: a tribute to Francis R (Joe) Boyd Geochem Soc Spec Publ 6:171–188

Smyth JR (1980) Cation vacancies and the crystal chemistry of breakdown reactions in kimberlitic omphacites. Am Mineral 65:1257–1264

Smyth JR, Caporuscio FA, McCormick TC (1989) Mantle eclogites: evidence of igneous fractionation in the mantle. Earth Planet Sci Lett 93:133–141

Snyder GA, Taylor LA, Crozaz G, Halliday AN, Beard BL, Sobolev VN, Sobolev NV (1997) The origins of Yakutian eclogite xenoliths. J Petrol 38:85–113

Sun S, McDonough WF (1989) Chemical and isotope systematics of oceanic basalts: implications for mantle composition and processes. In: Saunders AD, Norry MJ (eds) Magmatism in the ocean basins. Geol Soc Spec Publ 42:313–345

Switzer G, Melson WG (1969) Partially melted kyanite eclogite from the Roberts Victor Mine, South Africa. Smithsonian Contrib Earth Sci 1:1–9

Taylor WR (1998) An experimental test of some geothermometer and geobarometer formulations for upper mantle peridotites with application to the thermobarometry of fertile lherzolite and garnet websterite. Neues Jahr Miner Abh 172:381–408

Taylor LA, Neal CR (1989) Eclogites with oceanic crustal and mantle signatures from the Bellsbank kimberlite, South Africa, Part 1: mineralogy, petrography, and whole-rock chemistry. J Geol 97:551–567

Taylor LA, Snyder GA, Crozaz G, Sobolev VN, Yefimova ES, Sobolev NV (1996) Eclogitic inclusions in diamonds: evidence of complex mantle processes over time. Earth Planet Sci Lett 142:535–551

Taylor LA, Snyder GA, Keller R, Remley DA, Anand M, Wiesli R, Valley JW, Sobolev NV (2003) Petrogenesis of group A eclogites and websterites: evidence from the Obnazhennaya kimberlite, Yakutia. Contrib Mineral Petrol 145:424–443

Tollo RP (1982) Petrography and mineral chemistry of ultramafic and related mineral inclusions from the Orapa A/K-1 kimberlite pipe, Botswana. Dept Geol Geogr Contrib 39, Univ Massachusetts, Amherst

Viljoen KS (1994) The petrology and geochemistry of a suite of mantle-derived eclogite xenoliths from the Kaalvallei kimberlites, South Africa. Unpublished PhD thesis, Univ Witwatersrand

Viljoen KS, Smith CB, Sharp ZD (1996) Stable and radiogenic isotope study of eclogite xenoliths from the Orapa kimberlite, Botswana. Chem Geol 131:235–255

Wells PRA (1977) Pyroxene thermometry in simple and complex systems. Contrib Mineral Petrol 62:129–139